

# Advances in separation of monochiral semiconducting carbon nanotubes and the application in electronics

Cite as: J. Appl. Phys. 134, 230701 (2023); doi: 10.1063/5.0172970

Submitted: 19 August 2023 · Accepted: 12 November 2023 ·

Published Online: 18 December 2023



View Online



Export Citation



CrossMark

Yanan Sun,<sup>1,2</sup> Jiejie Zhu,<sup>2</sup> Wenhui Yi,<sup>3</sup> Yuxiang Wei,<sup>1,2</sup> Xuejiao Zhou,<sup>1,2</sup> Peng Zhang,<sup>2</sup> Yang Liu,<sup>1</sup> Peixian Li,<sup>1</sup> Yimin Lei,<sup>1,2,a)</sup> and Xiaohua Ma<sup>2,a)</sup>

## AFFILIATIONS

<sup>1</sup>School of Advanced Materials and Nanotechnology, Xidian University, Xi'an 710126, China

<sup>2</sup>State Key Laboratory of Wide-Bandgap Semiconductor Devices and Integrated Technology, School of Microelectronics, Xidian University, Xi'an 710071, People's Republic of China

<sup>3</sup>School of Electronics Science and Engineering, Faculty of Electronic and Information Engineering, Xi'an Jiaotong University, Xi'an 710049, Shaanxi, People's Republic of China

<sup>a)</sup>Authors to whom correspondence should be addressed: leiyim@xidian.edu.cn and xhma@xidian.edu.cn

## ABSTRACT

For over half a century, traditional silicon-based integrated circuits (ICs) have been the basis of computational electronics and are widely used in computers, cell phones, and other fields. With the rapid development of human society, silicon-based semiconductor technology is approaching its physical and engineering limits. Our increasing diversity of non-traditional computing needs, such as ultra-small, ultra-fast, ultra-low-power wearables, and space radiation protection, is driving the search for new electronic materials. Semiconducting single-walled carbon nanotubes (s-SWCNTs) have many excellent electrical properties, such as high carrier mobility and high ballistic transport, making them strong candidates for new semiconductor materials in the post-Moore era. Carbon-based electronic technology has been developed for over 20 years, and the fundamental issues such as the material purification of s-SWCNTs, preparation prospects of s-SWCNT-based field-effect transistors (CNT FETs), and device physics based on CNT FETs have been basically solved. However, the chiral diversity of s-SWCNTs may lead to problems such as fluctuations in the electrical performance of CNT FETs, limiting the application of s-SWCNTs in high-end ICs. Monochiral s-SWCNTs not only have excellent electrical properties but also have a controllable structure and uniformity, which are crucial for the high-end IC of CNTs. However, some problems exist in the purity and yield of monochiral s-SWCNT preparation and the optimization of monochiral CNT FETs. Therefore, the chiral sorting of CNTs is reviewed in this paper, and the progress of polymer reprocessing in chiral separation is highlighted. Then, the research progress of monochiral CNT FETs is introduced, and possible development directions are summarized and analyzed. Finally, the application prospects of chiral-enriched s-SWCNTs include challenges and future opportunities.

Published under an exclusive license by AIP Publishing. <https://doi.org/10.1063/5.0172970>

23 December 2023 06:45:12

## I. INTRODUCTION

The semiconductor industry's process technology has been gradually approaching its physical limits, so silicon-based semiconductors are becoming increasingly difficult to develop and manufacturing costs have risen dramatically. Therefore, in the post-Moore era, next-generation computing requires the exploration of new electronic materials. Semiconducting single-walled carbon nanotubes (s-SWCNTs) are one of the most promising electronic materials to replace silicon-based semiconductors due to

their outstanding properties such as quasi-one-dimensional structure, high carrier mobility, ultrathin channels, and high saturation velocity.<sup>1–7</sup> Semiconducting single-walled carbon nanotube-based field-effect transistors (CNT FETs) have shown great potential for applications in digital computing, radio frequency (RF) electronics, sensing, detection, 3D integrated circuits (ICs), etc.<sup>8,9</sup>

As one of the important technologies in the post-Moore era, carbon-based electronics has completed its early exploration. However, many problems must be solved before s-SWCNTs can be

further developed in high-end ICs. For example, one barrier is the structure and performance heterogeneity of s-SWCNTs. With the shrinking of the CNT FET size, there are a few s-SWCNTs with multiple chiral structures in the channel, resulting in an unstable electrical performance for CNT FETs. It is obvious that a monochiral s-SWCNT with controllable structures and homogeneous performance is critical for high-end applications of CNT FETs in the future.<sup>10</sup> Based on the above background, chiral sorting of s-SWCNTs is the bottleneck that needs to be addressed in carbon-based electronics. Nowadays, direct growth<sup>11</sup> and post-processing sorting<sup>12</sup> are two popular techniques to prepare monochiral s-SWCNT materials. However, the purity and corresponding CNT film are far from its intrinsic advantage. It is a long way for monochiral-based CNT FETs to meet the requirements of high-end IC applications accordingly.<sup>13</sup>

In this article, we review the research progress on the monochiral s-SWCNTs and corresponding CNT FETs: An introduction to the chirality of s-SWCNTs is provided first, including the overview of chiral sorting methods in which the polymer post-processing approach is highlighted. Then, an overview of the current research progress based on monochiral CNT FETs is highlighted, emphasizing the current development of CNT materials in radio frequency (RF) and flexibility. Finally, this review points out the challenges and development opportunities in the research of monochiral materials and their CNT FETs.

## II. CHIRAL SORTING

### A. Introduction to the chiral of SWCNTs

Due to the large aspect ratio, SWCNTs are often considered quasi-1D objects, which can be imagined as hollow cylinders formed by single-layer graphene rolled up in a certain orientation.<sup>3,14,15</sup> The graphene lattice vector is given by two integer indices  $(n,m)$  counting unit cells along the crystallographic  $(1,0)$  and  $(0,1)$  directions.<sup>16</sup> The chiral vector is defined as

$$C = n\alpha_1 + m\alpha_2 = (n, m), \quad (1)$$

where  $\alpha_1$  and  $\alpha_2$  are the basis vectors in the graphite lattice and  $(n,m)$  is the chiral index,<sup>17</sup> as shown in Fig. 1.<sup>18</sup> Their electronic conductivity has been predicted to depend sensitively on the tube diameter and the wrapping angle, with only slight differences in these parameters causing a shift from a metallic to a semiconducting state.<sup>17</sup> SWCNTs exhibit semiconducting properties when  $n-m = 3z \pm 1$  (where  $z$  is an integer) and metallic characteristics when  $n-m \neq 3z \pm 1$  (where  $z$  is an integer). The chiral indices  $(n,m)$  of the SWCNTs also directly determine their diameters as in the following equation:

$$D = \frac{a}{\pi} \sqrt{m^2 + n^2 + mn}, \quad (2)$$

where  $a$  is the length of the base vector. For s-SWCNTs, the bandgap is inversely proportional to the diameter, as in the

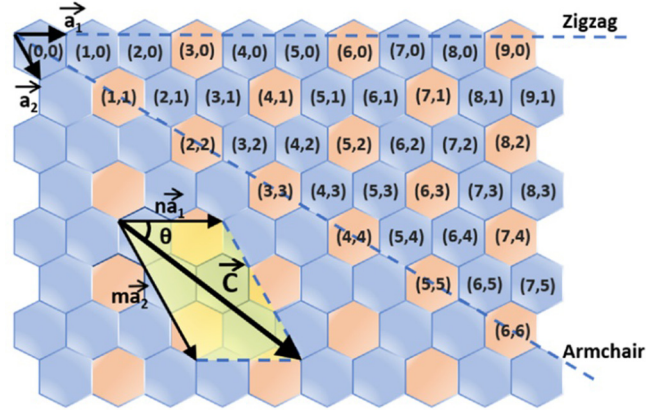


**FIG. 1.** Chirality map showing the structure of SWCNTs. Blue chiral indices represent the s-SWCNTs and orange chiral indices represent the metallic SWCNTs (m-SWCNTs). Approximately two-thirds of as-produced SWCNTs are semiconducting where  $\theta$  is the chiral angle.<sup>18</sup> Reproduced with permission from J. Y. Wang *et al.*, *Polymers* **12**, 1548 (2020). Copyright 2020 Author(s), licensed under a Creative Commons Attribution (CC BY) license.

following equation:

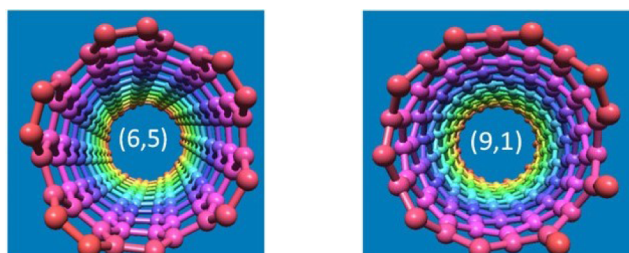
$$E_{\text{gap}} = \frac{2\gamma_0 a_0}{d_{\text{CNT}}}, \quad (3)$$

where  $\gamma_0$  is the integral exchange constant of carbon atoms,  $a_0$  is the shortest distance between carbon atoms, and  $d_{\text{CNT}}$  means the tube diameter.

SWCNTs can be categorized as armchair, zigzag, and chiral nanotubes according to  $\theta$ . If  $n$  is equal to  $m$ , SWCNTs are armchair nanotubes ( $\theta = 30^\circ$ ). If  $m$  is equal to 0, SWCNTs are zigzag nanotubes ( $\theta = 0^\circ$ ). Both the two types of SWCNTs are non-chiral tubes, while SWCNTs with  $n \neq m \neq 0$  are chiral nanotubes ( $\theta = 0^\circ - 30^\circ$ ). The "mod" refers to the congruence function. The mod (X, Y) equals the remainder of X divided by Y. According to the values of mod  $(2n + m, 3)$ , if the value is 1, the s-SWCNTs are categorized as type I. If the value is 2, the s-SWCNTs are categorized as type II.<sup>19</sup>

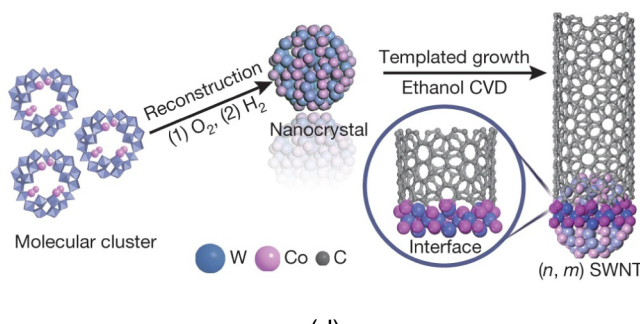
It is obvious that many properties of SWCNTs are related to chirality, such as electronic property,<sup>20–23</sup> optical property,<sup>24–26</sup> and thermal conductivity.<sup>2,27,28</sup> In particular, the charge transport properties of SWCNTs have been investigated in the field of ICs.<sup>5</sup> The electronic properties of SWCNTs vary with the chiral vector, as shown in Fig. 1, where the  $(n,m)$  values can represent whether the SWCNT is metallic or semiconducting. s-SWCNTs with semiconductor purity above 99% can be used in applications such as FET devices.<sup>3,6</sup> In addition, chirality also affects the optical properties of SWCNTs. Based on Kataura's study, the structure of carbon nanotubes affects their optical leaps,<sup>17</sup> which, in turn, affects the electroluminescence<sup>29</sup> and photoluminescence properties<sup>23,24</sup> of the devices. Chirality also determines the thermal conductivity<sup>30</sup> and mechanical properties<sup>17,31–34</sup> of SWCNTs. There is an increasing interest in the chiral studies of SWCNTs.

The s-SWCNTs contain a variety of chiral structures, and small differences in atomic arrangements lead to significant differences in bandgap structures. The chiral diversity affects the homogeneity of the transistor's electrical properties and limits the application of s-SWCNTs in high-end ICs.<sup>35</sup> This paper focuses on the research progress of chirality of s-SWCNTs in electronics. The single chiral s-SWCNTs have specific diameters, structures, bandgaps, and energy levels,<sup>36</sup> achieving material homogeneity. It also makes no contact barriers between carbon tubes, which is of great significance for transistor devices. Structurally controllable monochiral s-SWCNTs play a great role in the performance modulation and functional design for transistor devices. Therefore, one of the ultimate goals of carbon-based electronics is to use single chiral s-SWCNTs as channel materials.<sup>10</sup> After more than 20 years of exploration, researchers have developed a series of techniques for sorting s-SWCNTs according to diameter, length, electrical properties, and chirality,<sup>3,37</sup> including direct growth process, selective destruction process, and post-processing sorting. The article provides a systematic overview of the sorting methods of these three s-SWCNTs and focuses on the more common polymer post-processing sorting processes currently available. Some suggestions are given so that readers can obtain useful information.

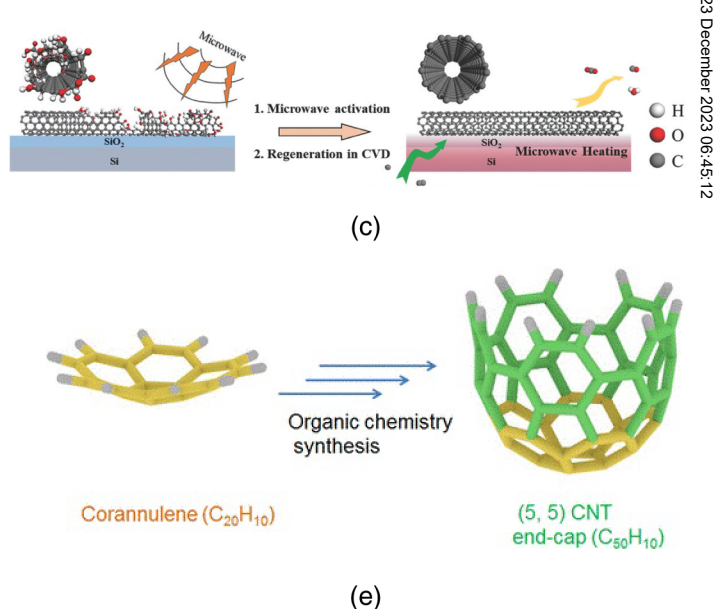


(a)

(b)



(d)



23 December 2023 06:45:12

**FIG. 2.** Structure of SWCNTs and recent major achievements on the chirality-controlled synthesis of SWCNTs. (a) and (b) Atomic structure of (6,5) and (9,1) s-SWCNTs, respectively.<sup>7</sup> Reproduced with permission from B. L. Liu *et al.*, ACS Nano **11**, 31–53 (2017). Copyright 2017 American Chemical Society. (c) Cloning of CNTs: Schematic showing the microwave-assisted regeneration of SWCNTs.<sup>45</sup> Reproduced with permission from D. W. Lin *et al.*, Small **14**, 1800033 (2018). Copyright 2018 John Wiley and Sons. (d) Preparation of the W-Co nanocrystal catalyst and the templated growth of a SWNT with specified  $(n, m)$ .<sup>46</sup> Reproduced with permission from F. Yang *et al.*, Nature **510**, 522 (2014). Copyright 2014 Springer Nature. (e) Structure of the molecular end-caps used for nanotube growth.<sup>44</sup> Reproduced with permission from B. L. Liu *et al.*, Nano Lett. **15**, 586–595 (2015). Copyright 2015 American Chemical Society. (Left) Structure of the bowl-shaped corannulene molecule ( $C_{20}H_{10}$ ) precursor. (Right) Structure of the hemispherical  $C_{50}H_{10}$  molecule synthesized from corannulene (a), which represents the end-cap plus a short sidewall segment of a (5,5) SWCNT.

The process also is known as “carbon nanotube cloning.”<sup>47</sup> As shown in Fig. 2(c), SWCNT fragments on a SiO<sub>2</sub>/Si substrate were activated by a microwave-assisted method, and then, the activated SWCNT with high regeneration efficiency was grown by CVD. This growth method enables micrometer-scale extension of SWCNTs.<sup>45</sup> Yao *et al.* obtained monochiral s-SWCNTs with a yield of 40% by adjusting the substrate material (e.g., quartz) and process temperature.<sup>48</sup>

- (b) Direct growth by metallic nanoparticles generally refers to the formation of high catalytically active metallic nanoparticle catalysts (e.g., Co, Fe, Ni, Cu, Ag, Au, Pd, Pt, and Mn) of designed sizes on a substrate and then the synthesis of SWCNTs through steps such as CVD, carbon adsorption, nucleation, and extension.<sup>5,49,50</sup> As shown in Fig. 2(d), Yang *et al.* used tungsten-based bimetallic alloy nanocrystalline catalysts for the direct growth of monochiral (12, 6) SWCNTs. Due to the use of high melting point catalysts, they obtained a highly stable round crystal structure during calcium carbonate deposition, which allowed the carbon atoms to be stably aligned around the single-walled carbon nanotubes and to form a good match with a certain crystalline surface of the catalyst. The chiral purity of monochiral (12,6) SWCNTs was as high as 92%.<sup>46</sup> Wu *et al.* developed Co-MgO catalysts, which formed stable Co nanoparticles upon reduction.<sup>51</sup> Under the condition of such stabilized nanoparticles, (6,5) species and (7,5) species were grown at reaction temperatures of 700 and 800 °C, respectively. Generally, SWCNTs prepared by this growth method are highly sensitive to the catalyst properties as well as other parameters of the growth process. Therefore, the ideal conditions for selective growth of monochiral SWCNTs are to simultaneously control a large number of growth parameters including the catalyst size and structure,<sup>52–54</sup> growth temperature,<sup>50–54</sup> and reaction promoter.<sup>55–59</sup>
- (c) Direct growth by carbonaceous molecular precursors generally refers to the preparation of carbonaceous templates (e.g., SWCNT end-cap precursors and carbon nanorings) on carbon-containing molecular precursors by bottom-up organic chemical synthesis. The prepared carbonaceous templates were then precipitated on quartz or silicon substrates and epitaxIALIZED into nearly pure s-SWCNTs by the gas phase.<sup>44</sup> Liu *et al.* reported that the characterization of SWCNTs revealed that their chirality changed during the growth process, despite the precise design of the precursors. This problem represents a challenge to the direct growth of carbon-containing molecular precursors. The pre-synthesized SWCNTs end-cap precursors and oxidation temperatures, etc., have an effect on the growth rate and chiral control of SWCNTs.<sup>44,60</sup> Even with these challenges, the method has many advantages, including metal-free catalyst growth and the potential for scalability through the use of the high-throughput organic synthesis of identical templates.<sup>7,44,49,60</sup> The researchers have explored various aspects of the catalysts, such as chemical composition, physical state, size, shape, and pretreatment conditions, to realize the increased chiral purity of monochiral SWCNTs.<sup>7</sup> However, the specific growth of SWCNTs with specific chirality including purity, yield, and growth rate<sup>5</sup> is difficult to control precisely. As the growth temperature increases, the catalyst particles may start to

produce thermal vibrations, which could prevent the growth of specific chirality for the growth of large-diameter SWCNTs.<sup>61</sup> Technological innovations for the growth of SWCNTs, such as further development of catalysts, process optimization of the growth process, and how to achieve low-cost mass production, are urgently needed to address the chiral selective growth of nanotubes.

## 2. Selective destruction processes

Unlike the direct growth process, the selective destruction process generally refers to the selective destruction of unwanted SWCNTs by electrical breakdown,<sup>62–64</sup> light-assisted breakdown,<sup>65–67</sup> plasma-assisted breakdown,<sup>68,69</sup> microwave-assisted breakdown,<sup>70,71</sup> and functionalization<sup>72,73</sup> to achieve the purpose. Typically, the selective destruction processes described above are separated primarily based on the difference in properties between s-SWCNTs and metallic SWCNTs (m-SWCNTs). This article summarizes five common selective destruction processes that readers can read for information.

- (a) Electrical breakdown generally refers to the etching of m-SWCNTs due to current-thermal effects<sup>61</sup> and the protection of s-SWCNTs due to electrostatic coupling<sup>62</sup> when passing currents of high current density, as shown in Fig. 3(a). This method is less costly but inevitably damages some of the s-SWCNTs during processing due to the effect of Joule heating of the current. This results in the enrichment of high-purity s-SWCNTs, although some auxiliary means (e.g., coating a 50 nm-thick organic film on the carbon nanotubes to destroy the m-SWCNTs to a greater extent by Joule heating<sup>64</sup>) are used, it is necessary to lose of most of the s-SWCNTs to achieve the target purity, and, thus, the yield of s-SWCNTs was low.
- (b) Light-assisted breakdown generally refers to the destruction of small-diameter m-SWCNTs by irradiation with a high-power long-arc xenon lamp or laser for a certain period of time to realize the enrichment of s-SWCNTs, as shown in Fig. 3(b).<sup>64</sup> Most of the m-SWCNTs are removed at the beginning of the process. As the time of irradiation increases, more and more s-SWCNTs are destroyed. In addition, factors such as time<sup>64,66,73</sup> and solvent<sup>82</sup> largely affect the removal of SWCNTs of specific chirality and diameter.
- (c) Plasma-assisted breakdown is the process of etching m-SWCNTs with plasma and retaining s-SWCNTs. It has been found that smaller SWCNTs are destroyed first during the etching process, so this method can improve the diameter distribution. In Fig. 3(c), SWCNTs with different diameters were compared after plasma etching at 400 °C and annealing at 600 °C.<sup>68</sup> During the etching process, metal nanoparticles (e.g., catalyst residues) are separated from the SWCNTs, which serves to clean the carbon tubes. Therefore, this method can be considered for post-processing to remove excess polymer residues.
- (d) Microwave-assisted breakdown is the process of removing m-SWCNTs by treating SWCNT raw materials with microwave radiation, as shown in Fig. 3(d).<sup>69</sup> This process not only optimizes the diameter distribution of carbon nanotubes and removes catalyst residues, but also makes it possible to use a

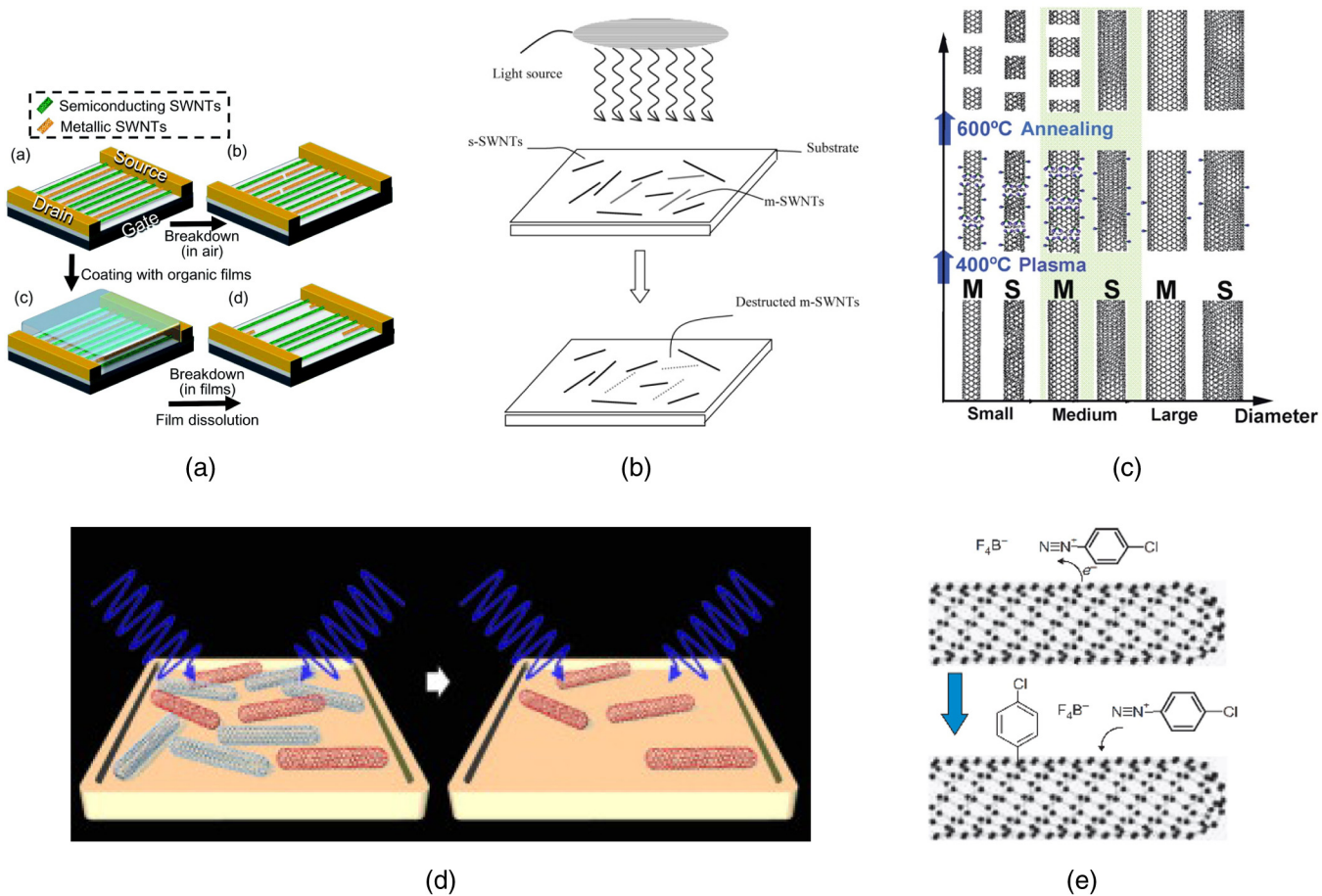


**FIG. 3.** (a) Schematic illustrations of (① and ②) electrical breakdown in air and (①, ③, and ④) electrical breakdown in organic films.<sup>64</sup> Reproduced with permission from K. Otsuka *et al.*, *Nanoscale* **6**, 8831–8835 (2014). Copyright 2014 Author(s), licensed under a Creative Commons Attribution (CC BY) license. (b) Schematic drawing of carbon nanotubes exposed to laser irradiation. Semiconducting carbon nanotubes (black) and metallic carbon nanotubes (gray) are illustrated.<sup>65</sup> Reproduced with permission from H. J. Huang *et al.*, *J. Phys. Chem. B* **110**, 7316–7320 (2006). Copyright 2006 American Chemical Society. (c) Schematic illustrations of plasma-assisted breakdown.<sup>66</sup> Reproduced with permission from G. Y. Zhang *et al.*, *Science* **314**, 974–977 (2006). Copyright 2006 AAAS. (d) Schematic illustrations of the microwave heating system for removing m-SWCNTs (blue ones).<sup>67</sup> Reproduced with permission from J. W. Song *et al.*, *Curr. Appl. Phys.* **8**, 725–728 (2008). Copyright 2008 Elsevier. (e) Schematic illustrations of functionalization.<sup>74</sup> Reproduced with permission from M. S. Strano *et al.*, *Science* **301**, 1519–1522 (2003). Copyright 2003 AAAS.

23 December 2023 06:45:12

household microwave oven as an experimental device. However, s-SWCNTs and m-SWCNTs cannot be effectively separated by this process, and more in-depth studies are needed.<sup>70</sup>

- (e) Functionalization is a way to introduce charged or charge-neutral functional groups to SWCNTs to enhance the differentiation of m-SWCNTs from s-SWCNTs for subsequent processing, as shown in Fig. 3(e).<sup>73</sup> It was found that the functionalization of m-SWCNTs with diazonium reagents facilitated separation by electrophoresis.

The selective destruction process is still in the early stage of chiral sorting, which cannot realize the enrichment of s-SWCNTs with specific chirality. On the one hand, it is necessary to optimize

the sorting process and improve the sorting mechanism. On the other hand, we can consider combining selective destruction with other processing methods in order to find a more superior way of chiral enrichment.

### 3. Post-processing sorting

Since the discovery of CNTs by Iijima in 1991, methods such as arc discharge, laser ablation, chemical vapor deposition (CVD), plasma torch, high-pressure carbon monoxide (HiPco) process, and the cobalt/molybdenum co-catalyst (CoMoCAT) process have been invented for the macro-preparation of carbon nanotubes.<sup>75–77</sup> Typically, the content of SWCNTs (a mixture of m-SWCNTs and s-SWCNTs) in large-scale prepared CNTs is about 30–70 wt. %,<sup>78</sup>

and the rest is other impurities such as amorphous carbon and catalyst. For example, SWCNTs prepared by HiPco have a diameter distribution of 0.7–1.1 nm and contain 45 different chiral species.<sup>79</sup> For most applications, only high-purity s-SWCNTs or m-SWCNTs are usually required. However, most of the SWCNTs usually consist of multiple chiral species, which has a significant negative impact on the device performance.

On the one hand, the diameters of commercially available mass-produced SWCNTs are distributed over a wide range. For example, SWCNTs prepared by CoMoCAT and HiPco processes have smaller diameters of 0.7–0.9 nm and 0.8–1.2 nm, respectively. SWCNTs prepared by plasma and arc discharge processes have larger diameters of 1.1–1.5 nm and 1.2–1.7 nm, respectively.<sup>78</sup> On the other hand, due to the high van der Waals attraction and p-p interactions between SWCNTs, the carbon tubes are easily “bundled” together and cannot be separated.<sup>80,81</sup> In this context, post-processing strategies such as density gradient ultracentrifugation (DGU),<sup>80,81</sup> DNA wrapping,<sup>82</sup> gel chromatography (GC),<sup>83</sup> dielectrophoresis,<sup>84</sup> aqueous two-phase extraction (ATPE),<sup>85</sup> and conjugated polymer wrapping<sup>86</sup> have been invented to sort SWCNTs based on different electronic properties, chiralities, and diameters.<sup>37</sup> This paper summarizes several of these reprocessing methods and focuses on the conjugated polymer wrapping process.

Density gradient ultracentrifugation (DGU) exploits differences in the buoyant densities (mass per volume) among SWCNTs of different structures. In this technique, purification is induced by ultracentrifugation in a density gradient. In response to the resulting centripetal force, particles sediment toward their respective buoyant densities and spatially separate in the gradient.<sup>87</sup> As shown in Fig. 4(a) (right), SWCNTs form isolated colored bands arranged by diameter and chirality. Only SWCNTs with different electron types and diameters could be separated by DGU at the beginning of the study, and after more in-depth exploration, chirality-based sorting of SWCNTs was also realized by the orthogonal iteration of DGU.<sup>79</sup> However, the expensive density gradient media and time-consuming separation process limit the industrialization of DGU.

DNA wrapping utilizes the  $\pi$ -stacking effect between single-stranded DNA (ssDNA) and bundled SWCNTs, which causes bundled SWCNTs to be helically wrapped<sup>82</sup> by ssDNA. Therefore, the bundled SWCNTs can be efficiently dispersed in water during sonication, as shown in Figs. 4(b) and 4(c). The binding free energy of ssDNA to carbon nanotubes rivals that of two nanotubes for each other. By rational sequence and structure design of ssDNA, it can disperse monochiral SWCNTs.<sup>88</sup> However, this technique is greatly influenced by the source of raw materials (mainly SWCNTs prepared by HiPco),<sup>82</sup> so it is mainly used for the isolation of small-diameter SWCNTs at present. In addition, the cost of dispersion is too high for large-scale preparation.<sup>88</sup>

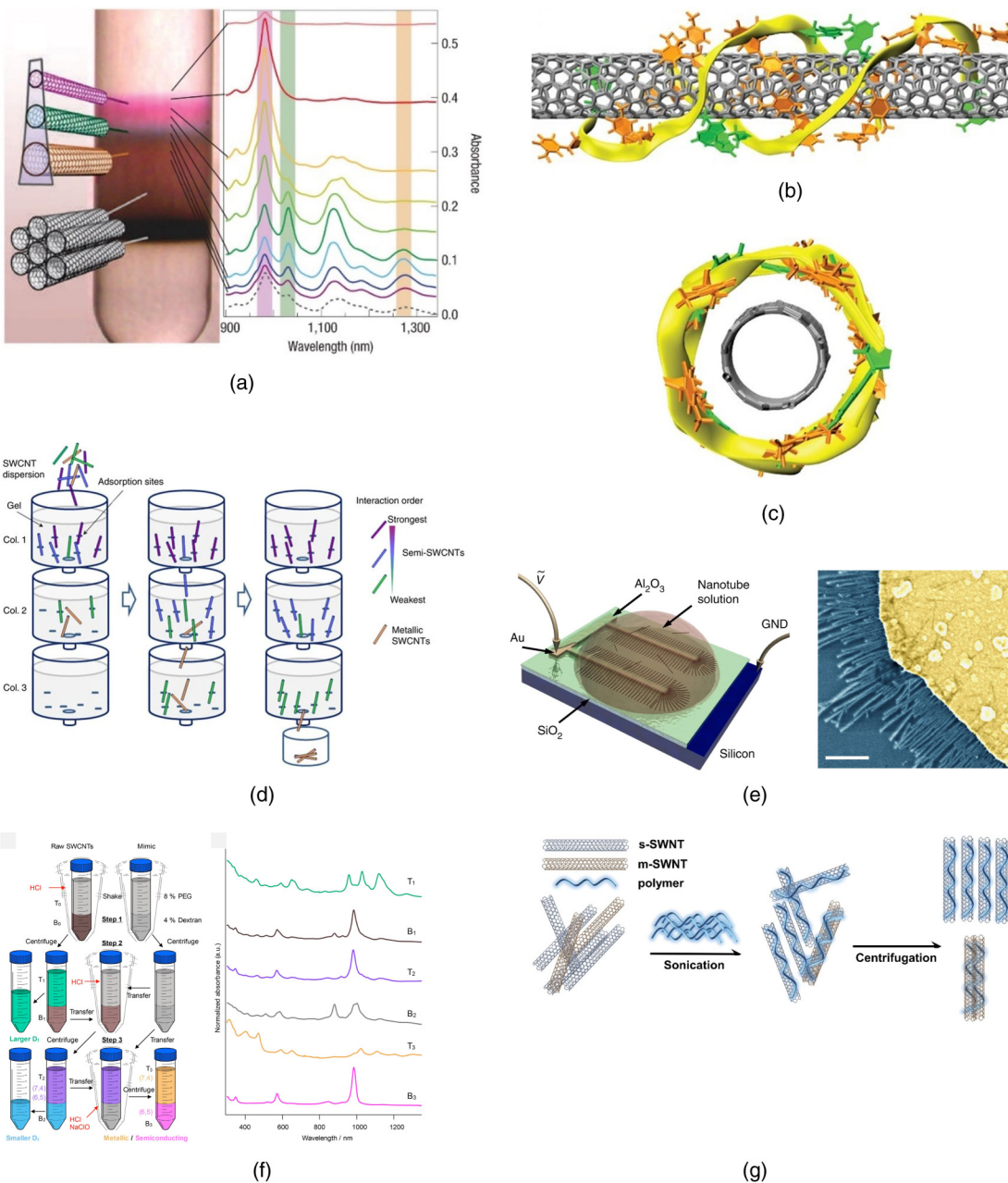
Gel chromatography (GC) is a method that utilizes selective interactions between SWCNT species and various stationary phases to separate SWCNT dispersions as they pass top-down through a series of vertically connected gel columns.<sup>83</sup> As shown in Fig. 4(d). By choosing reasonable surfactant and gel columns,<sup>91</sup> GC can be used to separate SWCNTs with different lengths,

electron types, and chiralities. Liu *et al.* obtained 13 different chiral species SWCNTs with purities ranging from 39% to 94% by multiple separations using sodium dodecyl sulfate (SDS) as a dispersant.<sup>83</sup> By refining the solution preparation step with several iterations, Tulevski *et al.* obtained s-SWCNTs with purities up to 99.9%,<sup>92</sup> making it possible to use GC for the isolation of high-purity s-SWCNTs required for high-performance electronic devices. In recent years, GC has made new progress in the post-treatment of single chiral SWCNTs. Yang *et al.* tuned the selective adsorption of the gel medium by controlling the temperature of the sodium cholate (SC) and sodium dodecyl sulfate (SDS) binary surfactant system. The separation of 11 near zigzag monochiral SWCNTs was realized at temperatures below 18 °C.<sup>93</sup> Zanoni *et al.* found that different hydrogels have a strong effect on the chiral selectivity of SWCNTs. For example, Sephadryl S-200 was highly selective for (6,5) species, but Superose 6 adsorbed more SWCNTs than Sephadryl S-200 per unit area of the gel surface and was more selective for (7,3) and (7,5) species.<sup>94</sup> Dolan *et al.* investigated the role of hydrogels containing different ammonium persulfate (APS) concentrations in the purification of SWCNTs, laying the foundation for further optimization of gel media.<sup>95</sup> Luo *et al.* achieved selective adsorption and desorption of SWCNTs on a gel column by controlling the concentration of a novel sodium deoxycholate (SHC) surfactant and separated (6,5) species with chiral purity up to 97%.<sup>96</sup> These results indicate that gel chromatography has advantages in the purity and variety of monochiral SWCNT separation, which deserves an in-depth study by scientists.

Dielectrophoresis is a technique in which an AC voltage is applied to planar microelectrodes, causing an inhomogeneous electric field between the electrodes. Due to the different induced dipole moments between s-SWCNTs and m-SWCNTs, s-SWCNTs suspended in the solution near the electrodes selectively interact with the inhomogeneous electric field and are, thus, preferentially deposited.<sup>84</sup> Cao *et al.* found that stochastic hydrodynamic and Brownian motions affect the alignment of SWCNTs, and the arrays of SWCNTs prepared by electrophoresis usually suffer from bending and wobbling defects.<sup>77,82</sup> Recently, they obtained uniformly aligned SWCNT arrays by optimizing the edge electric field, as shown in Fig. 4(e).

Although the purity of s-SWCNTs prepared by dielectrophoresis was as high as 98%,<sup>97</sup> there was no evidence that dielectrophoresis contributed much to chiral sorting. It is possible that dielectrophoresis is more suitable for aligning and calibrating SWCNT spacing in order to prepare s-SWCNT array films with excellent performance.

Aqueous two-phase extraction (ATPE) is a commonly used method for the separation of SWCNTs, which involves the spontaneous formation of two immiscible aqueous phases by mixing polyethylene glycol (PEG) and dextrose anhydride (DEX) solutions. The separation of SWCNTs is achieved due to the different affinities of each aqueous phase for SWCNTs.<sup>85</sup> The affinity of the PEG/DEX system for different SWCNTs depends on factors such as the diameter, length, electron type, chirality, and surface chemistry (e.g., surfactant) of the SWCNTs.<sup>3</sup> Recent studies have shown the successful isolation of 11 different monochiral SWCNTs after three steps in ATPE using the PEG/DEX system. The



23 December 2023 06:45:12

**FIG. 4.** (a) Sorting of SWNTs by diameter, bandgap, and electronic type using DGU.<sup>87</sup> Reproduced with permission from M. S. Arnold *et al.*, Nat. Nanotechnol. **1**, 60–65 (2006). Copyright 2006 Springer Nature. (b) A DNA barrel on a (8,4) nanotube formed by rolling up a 2D DNA sheet composed of two hydrogen-bonded anti-parallel ATTTATTTATT strands.<sup>83,88</sup> Reproduced with permission from X. M. Tu *et al.*, Nature **460**, 250–253 (2009). Copyright 2009 Springer Nature. (c) The structure in (b) viewed along the tube axis. Color coding: orange, thymine; green, adenine; yellow ribbons, backbones.<sup>88</sup> Reproduced with permission from X. M. Tu *et al.*, Nature **460**, 250–253 (2009). Copyright 2009 Springer Nature. (d) Schematic diagram of single-surfactant multicolumn gel chromatography for separating SWCNTs.<sup>83</sup> Reproduced with permission from H. P. Liu *et al.*, Nat. Commun. **2**, 309 (2011). Copyright 2011 Author(s), licensed under a Creative Commons Attribution (CC BY) license. (e) Microscopic characterizations of the nanotube arrays assembled using the fringing-field dielectrophoresis.<sup>89</sup> Reproduced with permission from Q. Cao *et al.*, Nat. Commun. **5**, 5071 (2014). Copyright 2014 Springer Nature. (f) ATPE experimental procedure for the simultaneous three-step separation of 11 different chiral SWCNTs from the CoMoCAT raw material.<sup>90</sup> Reproduced with permission from H. Li *et al.*, ACS Nano **13**, 2567–2578 (2019). Copyright 2019 American Chemical Society. (g) Basic process of the conjugated polymer wrapping method for selectively dispersing s-SWNTs.<sup>18</sup> Reproduced with permission from J. Y. Wang *et al.*, Polymers **12**, 1548 (2020). Copyright 2020 Author(s), licensed under a Creative Commons Attribution (CC BY) license.

diameters of these SWCNTs were in the range of 0.69–0.91 nm<sup>80</sup> as shown in Fig. 4(f). Xu *et al.* isolated high-purity (6,5) and (7,5) species by ATPE and prepared multiple monochiral CNT devices.<sup>88</sup> Podlesny *et al.* found a way to further enrich monochiral SWCNTs by introducing a nonionic triblock copolymer surfactant into the system, which successfully increased the chiral purity of (6,5) and (7,5) SWCNTs.<sup>3,99</sup> The method they developed is capable of separating the monochiral fraction from polydisperse mixtures of SWCNTs, but this method is more suitable for the separation of small-diameter carbon tubes.<sup>100</sup> Usually, the ATPE method is used for the separation of small-diameter SWCNTs, and there is still difficulty in the separation of large-diameter SWCNTs. However, by adjusting the temperature<sup>101,102</sup> in the separation process and adding reasonable surfactants (e.g., NaSCN<sup>85</sup> and NaCl),<sup>103</sup> the ATPE method can be used for the separation of monochiral large-diameter SWCNTs.<sup>100</sup> Overall, compared with other existing methods for SWCNT separation, the ATPE method has the advantages of rapid separation and low cost.<sup>85,104,105</sup> However, more in-depth research is needed on how to improve the chiral purity.

Conjugated polymer wrapping refers to dispersing a mixture of SWCNTs and polymers in an organic solvent (e.g., toluene<sup>106</sup>), and ultrasonic waves are utilized to disperse the polymer-wrapped SWCNTs. Impurities and metal tubes are then precipitated by high-speed centrifugation.<sup>18</sup> Due to the strong polarizability of m-SWCNTs, m-SWCNT/polymer complexes have a stronger charge transfer than s-SWCNT/polymer complexes. Therefore, the more polar m-SWCNT/polymer complexes tend to aggregate in nonpolar solvents and form deposits after centrifugation, whereas the polymer-coated s-SWCNTs are retained in the supernatants,<sup>107,108</sup> as in Fig. 4(g). Although there are many

post-processing methods invented for sorting and purifying SWCNTs, a growing number of studies have shown that polymer post-processing is a method of enrichment of SWCNTs that provides higher yields (>20%) and higher purity (>99.9%),<sup>70,73,101–103</sup> and is more economical (requiring simpler equipment, operation, and shorter processing times).<sup>109</sup> Through unremitting efforts, researchers have developed many polymers with unique features for s-SWCNTs sorting, such as polymers that enable ultrahigh-purity electron-type enrichment,<sup>91,110</sup> low-cost recyclable polymers (e.g., photodegradation,<sup>111,112</sup> acid depolymerization,<sup>113–115</sup> high-temperature depolymerization,<sup>112</sup> and conformational changes<sup>116–119</sup>). A schematic of a process for sorting s-SWCNTs that can be used for acid depolymerization is given in Fig. 5.

The s-SWCNTs prepared by the conjugated polymer method can not only achieve ultrahigh semiconductor purity but also prepare high-purity, uniformly aligned films, which have become the preferred choice for the latest circuit applications.<sup>120,121</sup> By sorting raw CNTs with the polymer PCz {poly [9-(1-octyloxy)-9H-carbazole2,7-diyl]}, Peng's team achieved extremely high semiconducting purity higher than 99.9999% after multiple dispersions. It can be used to prepare wafer-scale s-SWCNT arrays with high directional density [controlled density (100–200/ $\mu\text{m}$ )] for high-performance electronic products.<sup>121</sup> However, the selective separation of monochiral s-SWCNTs still faces problems such as low purity. Therefore, how to continue the advantages of the conjugated polymer method in the post-processing of s-SWCNTs, improve the chiral purity and yield, reduce the cost, optimize the process, and realize the large-scale

23 December 2023 06:45:12

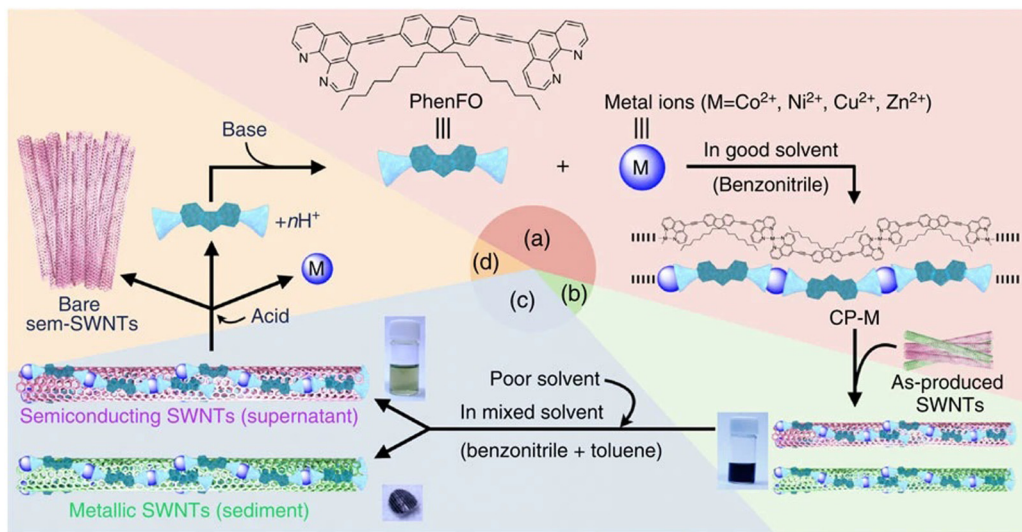


**FIG. 5.** A method for s-SWCNT sorting using removable solubilizers.<sup>114</sup> The purification method starts from (a) the preparation of CP-M (M %Co, Ni, Cu, and Zn), (b) solubilization of as-produced SWNTs, (c) separation of sem- and met-SWNTs, and (d) removal and recovery of the adsorbents. Chemical structure of PhenFO is shown in step (a). Reproduced with permission from F. Toshimitsu *et al.*, Nat. Commun. 5, 5041 (2014). Copyright 2014 Springer Nature.

industrialization of the preparation of monochiral s-SWCNTs are the problems that urgently need to be solved.

#### 4. Polymer wrapping separation

The composition of raw CNTs obtained by large-scale preparation is complex, containing CNTs with different diameters and impurities, and a variety of chiral species are mixed in the CNTs.<sup>78,109</sup> The properties of the polymers, such as molecular weight size, main chain structure, and side chain structure, have a great influence on the chiral sorting of s-SWCNTs.<sup>3,16,100</sup> Therefore, there is a need to understand the mechanism of chiral selectivity of CNTs wrapped in conjugated polymers, which is also important for the development of novel polymers with more chiral selectivity and optimization of the s-SWCNT sorting process. Liu *et al.* compared the chiral selectivity of poly[9,9-diptylfluorene-2,7-diyl]-alt(6,6'-{2,2'-bipyridine}) (PFO-BPy) and poly[9-(1-octyloxy)-9H carbazole-2,7-diyl] (PCz) for three commercially available raw materials for SWCNTs (CoMoCAT, HiPco, and arc discharge) with diameter distributions of 0.6–1.8 nm.<sup>122</sup> The two polymers have different geometries and different polymer–carbon nanotube interactions, so they have different chiral angles and diameter selections for different raw materials. They summarized many laws for sorting monochiral s-SWCNTs with polymers. For example, PFO-BPy selects fewer chiral species in small-diameter (<1 nm) s-SWCNTs and more chiral species in large-diameter (>1.2 nm) s-SWCNTs. Ozawa *et al.* used SWCNTs prepared by

CoMoCAT as the original material and continuously adjusted the type of polymer and solvent. Finally, the smaller diameter (6,5) s-SWCNTs were selectively enriched by PFO-BPy in “one-pot” (only sonication), and the chiral purity of the sorted (6,5) species reached 96%–97%.<sup>123</sup> Liu *et al.* similarly sorted s-SWCNTs prepared by CoMoCAT, and the (6,5)s-SWCNTs extracted with PFO-BPy were close to monochiral, with a chiral purity of >99%,<sup>122</sup> which reached a very desirable purity. Ouyang *et al.* matched a variety of s-SWCNTs and conjugated polymers separately by using a multi-cycle conjugated polymer extraction (CPE) method, and they found that the chiral selectivity of polymers for carbon tubes changes after multiple enrichment cycles, and, thus, specific chiral purity can be improved by this method.<sup>124</sup>

The chiral enrichment of s-SWCNTs by different polymers is different, and there may be “intersection” and “complementation.” Therefore, it is also possible to obtain nearly monochiral s-SWCNTs through a reasonable combination of polymers with different ultracentrifugation parameters.<sup>18,106,123,125–129</sup> For example, Li *et al.* used poly(9,9-diptylfluorene-2,7-diyl- alt-pyridine-2,6-diyl) (PFP) and poly[9-(1-octyloxy)-9H-carbazole-2,7-diyl-alt-pyridine-2,6-diyl] (PCP) polymers to encapsulate and disperse s-SWCNTs, combined with enhanced ultracentrifugation (E-UCG) and step-by-step extraction processing (STEP), to obtain (10,8) and (12,5) species with purities as high as 92.3% and 95.6%,<sup>126</sup> as shown in Fig. 6. They utilized thin films of (10,8) s-SWCNTs to make micro- and nanoscale FETs devices, which

23 December 2023 06:45:12

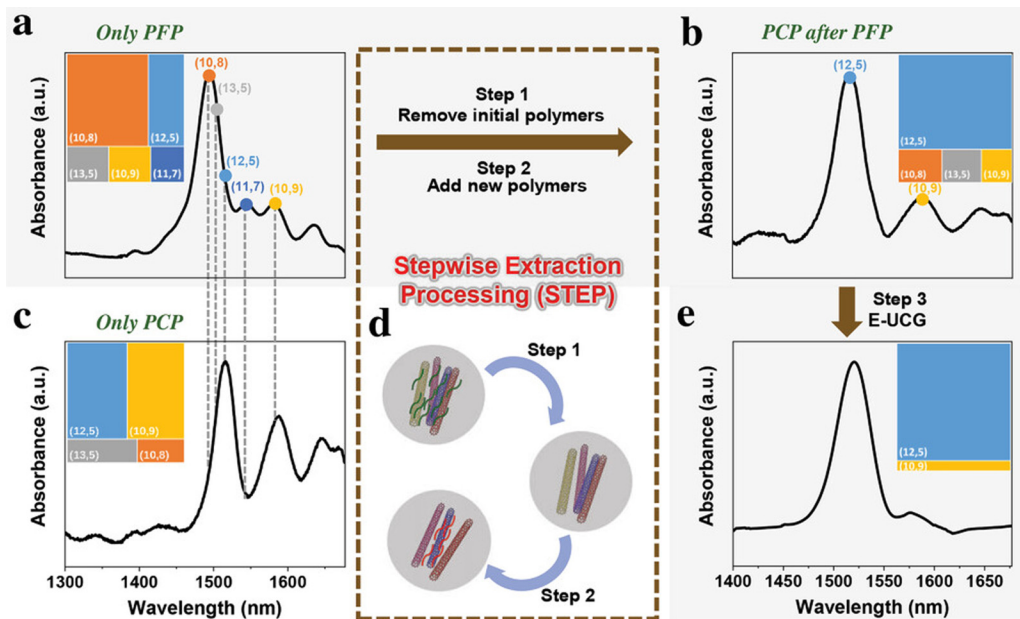


**FIG. 6.** Illustration of the (12,5) SWCNTs purified by stepwise extraction processing.<sup>126</sup> (a) and (c) S11 region of the absorption spectra of monochiral SWCNTs sorted by PFP and PCP, respectively. (b) S11 region of the absorption spectra of SWCNTs sorted by PCP following PFP. (d) Alternating process of polymers wrapping the surface of carbon tubes. (e) S11 region of the absorption spectra after E-UCG. The tree map charts in (a)–(c) and (e) represent the purity of different chiral species, which was confirmed by Lorentz fitting of the absorption spectra. Reproduced with permission from Y. H. Li *et al.*, *Adv. Funct. Mater.* **32**, 2107119 (2022). Copyright 2022 John Wiley and Sons.

exhibited on/off ratios up to  $10^6$  and carrier mobilities up to  $61 \text{ cm}^2 \text{ V}^{-1} \text{ s}^{-1}$ . According to their theory, there are intersecting and complementary situations in the sorting results of s-SWCNTs by different polymers. However, when using this method, care should be taken to remove the polymer residues to avoid affecting the later sorting process. Not only polymers but also dispersant molecules such as surfactants and DNA will remain on the surface of the isolated s-SWCNTs. The low conductivity and scattering effects of these dispersants increase the contact resistance between the nanotubes and the electrodes, thus greatly reducing the device performance. Various techniques have been developed to remove dispersant molecules, including rinsing, filtration, oxidation, and annealing. Recently, Li Qingwen *et al.* developed a rapid annealing and cooling method to clean s-SWCNT films,<sup>130</sup> which can completely remove the residual polymers on the surface of s-SWCNTs and effectively reduce the contact resistance between the metal electrode and the nanotubes. Compared with the films rinsed with organic solvents, the electrical properties of the s-SWCNTs films cleaned by this method were significantly improved, with a 700% reduction in the contact resistance between the nanotubes and the electrodes, and a 600% increase in the on-current of the CNT thin-film transistors (TFTs), which provided a more ideal solution to the problem of dispersant removal.

When the polymer/SWCNT ratio is small, only specific types of s-SWCNTs can be well encapsulated and dispersed. Other chiral s-SWCNTs cannot be efficiently encapsulated and, thus, tend to aggregate and bind together. Therefore, adjusting the appropriate polymer/CNT ratio facilitates the sorting of monochiral s-SWCNTs.<sup>3,16,100,115</sup> Nearly monochiral (7,6) s-SWCNTs with 90% chiral purity were obtained by dispersing 10 mg of poly(9,9-di-n-dodecylfluorene) (PFDD) and 10 mg of the SWCNT in 70 ml of toluene by Stuerzl *et al.* When an excess of PFDD was used (when the PFDD/SWCNT ratio was decreased), the sorted chirality was more complex, containing (7,5), (8,6) and (8,7)s-SWCNTs.<sup>128</sup>

The monochiral enrichment of s-SWCNTs can also be improved by adjusting the centrifuge speed and centrifugation time.<sup>126,131</sup> However, this may cause irreversible structural damage to s-SWCNTs, thus affecting their electrical, thermal, and optical properties. The monochiral enrichment of s-SWCNTs can also be improved by adjusting the centrifuge speed and centrifugation time.<sup>126,131</sup> However, this may cause irreversible structural damage to s-SWCNTs, thus affecting their electrical, thermal, and optical properties. Rother *et al.* selected a mixture of s-SWCNTs prepared by CoMoCAT as the raw material and separated it with polymer PFO at different centrifugation parameters, which resulted in nearly monochiral (7, 5) s-SWCNTs with purity up to 96%.<sup>106</sup> They pointed out that large-diameter, small-bandgap s-SWCNTs can preferentially transmit current, which is conducive to obtaining a large on-state current density.

The high cost of polymers has limited the industrialization of polymer inclusion separation methods. Recently, Wieland *et al.* have estimated the cost of polymer wrapping separation and ATPE method for sorting (6, 5) s-SWCNTs based on the prices of commercially available raw materials, dispersants, and solvents for s-SWCNTs.<sup>132</sup> Under laboratory conditions, the cost of separating 1 g of (6,5) s-SWCNTs by polymer encapsulation is as high as 36,000–73,000 euros, and the cost of the same separation of 1 g of

(6,5) s-SWCNTs by the ATPE method is only 8300–13,000 euros. Costs under laboratory conditions may decrease as synthesis and separation processes are optimized. The development of direct growth methods with controlled chirality is also important, but selective growth of all chiral species is difficult. Thus, the growth and post-processing sorting of monochiral SWCNTs will continue to be synergistic rather than one being the solution to the other in industrial production.<sup>12</sup>

Obviously, by choosing suitable raw CNTs and different conjugated polymers (possibly multiple), controlling a reasonable polymer/SWCNT ratio and suitable temperature, and performing high-speed centrifugation at different rotational speeds for different times and multiple iterations (even in combination with other post-processing modalities), we can obtain nearly monochiral s-SWCNTs. The preparation of high-purity, nearly monochiral s-SWCNTs network thin films is possible.<sup>89</sup> However, only six reported polymers have shown effective monochiral selectivity to date.<sup>81,123,127,133–135</sup> Designing polymer structures with high monochiral selectivity and perfecting the polymer wrapping separation process are urgent problems to be solved.<sup>136</sup> Some of the research progresses are summarized in Table I.

### III. ADVANCES IN CHIRAL-ENRICHED SWCNTs FIELD-EFFECT TRANSISTOR RESEARCH

Existing studies have made more progress in purification by the polymer wrapping method,<sup>138</sup> CNT arrangement,<sup>19,110,139–142</sup> and preparation process.<sup>143</sup> The carrier mobility of s-SWCNT FETs fabricated in networked or arrayed films ranges from tens to thousands of  $\text{cm}^2 \text{ V}^{-1} \text{ s}^{-1}$ ,<sup>137,139,144,145</sup> while the on/off ratio can be as high as  $10^8$ .<sup>146,147</sup> In order to further utilize the advantages of s-SWCNTs in high-performance IC applications, researchers have gradually begun to explore different chiral-enriched cases of s-SWCNT applications, such as chiral-enriched CNT FETs, chiral-enriched s-SWCNT photoemitters,<sup>148</sup> chiral-enriched s-SWCNT photodetectors,<sup>149</sup> and chiral-enriched s-SWCNT photovoltaic ICs.<sup>150</sup> Among them, FET, as the basic unit of an IC, performance directly determines the height and breadth of CNT applications. In the following, we focus on single chiral s-SWCNTs for FET applications.

#### A. Films of monochiral s-SWCNTs

Compared with other organic semiconductor materials, s-SWCNTs have excellent material intrinsic advantages. CNT FETs showed excellent electrical performance with bipolar transport, high on/off current ratio, negligible hysteresis, and high carrier migration.<sup>151</sup> However, due to the mixed structure of large-scale prepared CNTs, the structural diversity leads to the electrical properties of their prepared devices are often difficult to control,<sup>127</sup> which greatly affects the yield and reproducibility of large-scale ICs. Therefore, it is necessary to study the relationship between the chiral structure of CNTs and the device performance, and the effective identification of the chiral structure of CNTs is the basis for the in-depth study of the properties of CNTs and the expansion of the applications of CNTs.<sup>13</sup>

CNT film is the most mature CNT material for scalable fabrication of transistors and ICs. Thin-film transistors (TFTs) prepared

**TABLE I.** Advances in monochiral s-SWCNTs prepared by polymer wrapping method.

CNT sample	Polymer	SWCNT after screening				
		Chiral purity	Diameters (nm)	Bandgaps (eV)	Mobilities [cm <sup>2</sup> / (V s)]	Others
HiPco	PFO	(7,5)—19% (7,6)—21% (8,6)—28% (8,7)—26% (9,7) —6%	50.8–1.2	1.1–0.8	5–12	106
CoMoCat	PFO	(7,5)—96% (7,6) —4%	0.7–0.9	1.2–1.1	1–3	...
Arc Discharge	F8BT	(15,4) (15,5) (13,5)	1.3–1.6	0.8–0.6	20–60	134
CoMoCAT	PFO-BPy	(6,5)—96%–97%	0.7–0.9	1.2–1.1	1–3	123
Laser vaporization	PFDD	(10,9)	1.29	0.8	27	137
HiPco	PFP	(10,8)—92.3%	1.24	0.8	61	126
HiPco	PFP, PCP	(12,5)—95.6%	1.20	0.8	...	...
HiPco	Poly[(9,9-didodecylfluorenyl-2,7-diyl)] (PDDF)	(7,6)—90%	...	...	...	128
CoMoCAT	PFO-BPy	(6,5)—99%	0.6–1.0	1.2–1.1	...	122
CoMoCAT	PCz	(7,5)—75%	0.6–1.8	...	...	122

with high semiconductor purity SWCNTs are the basic unit of the semiconductor industry. On the one hand, high-purity monochiral s-SWCNTs have better electrical homogeneity of the prepared films due to their structural unity. On the other hand, the energy band structure of s-SWCNTs is determined by the atomic arrangement, which implies that the electrical properties of s-SWCNTs with different chiralities are different, and, thus, the performance of TFTs prepared from s-SWCNTs with different chiral structures varies greatly. Su *et al.* prepared 11 s-SWCNTs with different chiralities into thin films by a newly developed alkaline small molecule modulation technique<sup>152</sup> and then compared the performance differences of the corresponding TFTs, as shown in Fig. 7. They found that even for s-SWCNTs with the same diameter, the difference in on-state current or carrier mobility may reach an order of magnitude with different chiral angles. They also found that type I s-SWCNTs exhibited higher on-state current and higher carrier mobility with increasing chiral angle in the same family, while type II s-SWCNTs showed the opposite trend.<sup>35</sup> The structural controllability of monochiral s-SWCNTs is crucial for the performance modulation and functional design of transistor devices, and their results provide an important reference for the design of high-performance electronic devices based on monochiral s-SWCNTs.

## B. Factors affecting the quality of s-SWCNT films

### 1. Effect of chiral dispersion and tube size distribution on the quality of s-SWCNT films

Due to the chiral dispersion of the s-SWCNT solution, the diameter of the tube distribution is in the range of 0.8–1.7 nm,

which leads to a bandgap distribution in the range of 0.5–1 eV. On the one hand, bandgap variations lead to changes in contact behavior (ohmic contacts and Schottky barriers),<sup>153</sup> which further affects the on/off ratios, on-state resistances, charge injection, and threshold voltages of the s-SWCNT-based FETs,<sup>154</sup> as the s-SWCNT-based FETs perform charge transfer through a network of s-SWCNTs in thin films. As the size of the CNT FETs is further reduced (e.g., less than 10 nm), there are only a few s-SWCNTs in the channel. In this case, the diversity of chiralities in terms of energy levels, injection barriers, and threshold voltages will lead to a variation in the performance of individual s-SWCNT FETs.<sup>6,140</sup> On the other hand, Rother *et al.* showed that charge transport is mainly through CNTs with the smaller bandgap, even though they are only a small part of the network. CNTs with the largest bandgap only begin to participate in current transport at higher gate voltages.<sup>106</sup> Tulevsky *et al.* demonstrated that s-SWCNTs with tube diameters larger than 1.2 nm are suitable for FET devices, exhibiting significantly higher carrier mobility in CNT FET devices than small-diameter s-SWCNTs.<sup>135,141</sup> As shown in Fig. 8, Zhang *et al.* fabricated nanoelectronic devices with (10,5) species; the performance of the FETs made with the slightly bigger (10,5) tubes is better than their previously reported results using (7,6) and (8,4) tubes. Moreover, the large-diameter s-SWCNTs have good ohmic contacts with the metal electrodes.<sup>155</sup> In 2013, Maria Antonietta Loi separated large-diameter s-SWCNTs by poly(9,9-di-n-dodecylfluorene-2,7-diyl) (PF12), and the hole and electron mobilities of FETs prepared with such large-diameter s-SWCNTs were 14.3 and 16.4 cm<sup>2</sup> V<sup>-1</sup> s<sup>-1</sup>, respectively, and both of them were able to achieve an on/off ratio of 10<sup>5</sup>.<sup>156</sup> In 2020, Li Qingwen *et al.* utilized

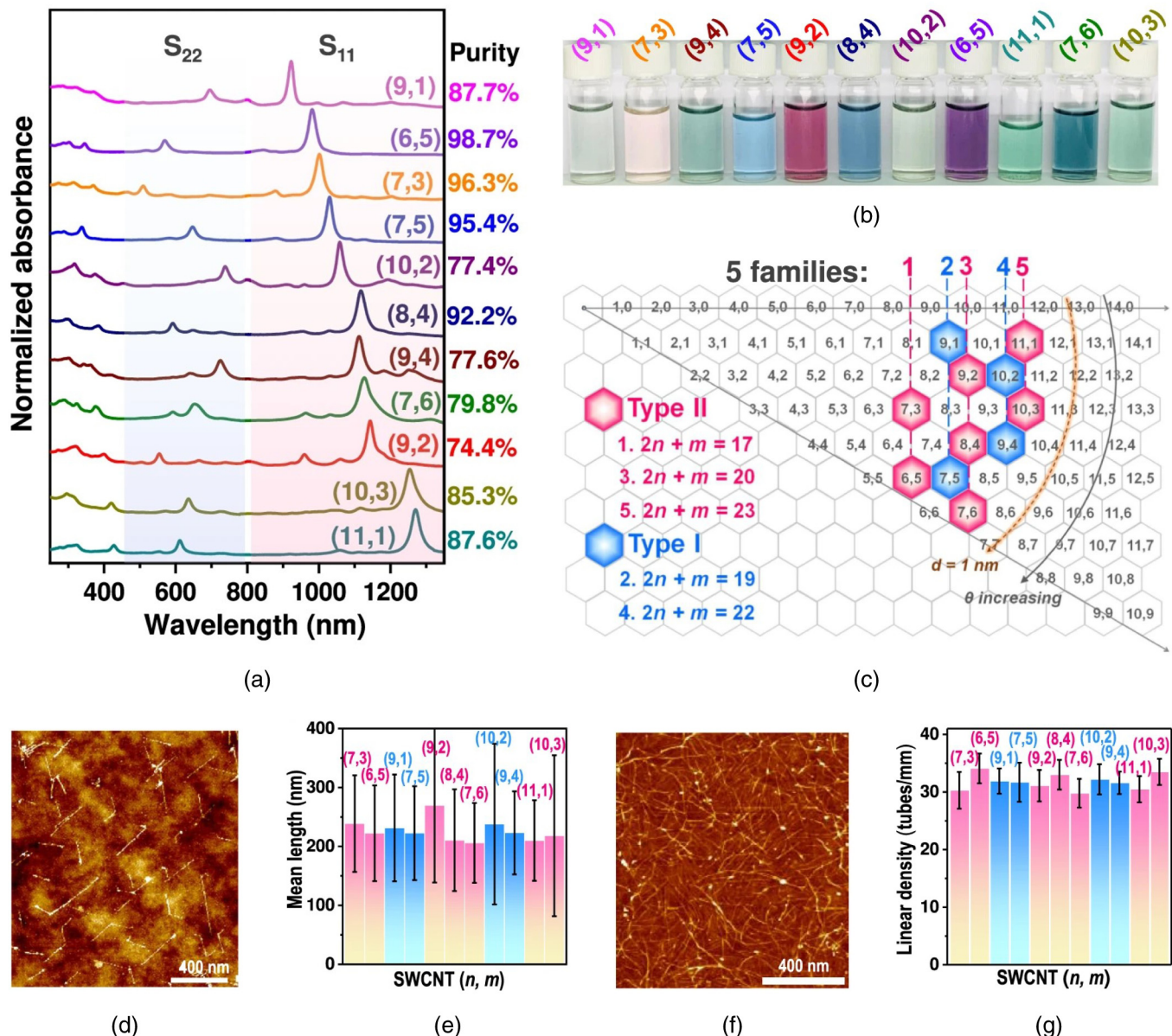


**FIG. 7.** (a) Optical absorption spectra of the  $(n,m)$  monochirality s-SWCNTs.<sup>35</sup> Their chiral purities are evaluated by peak fitting and indicated on the right-hand side. (b) Photographs of the monochirality s-SWCNT solutions. (c) Location of the monochirality s-SWCNTs in the chiral map. (d) Typical atomic force microscopy (AFM) image of a low-density s-SWCNT film for length measurement. (e) Statistical distribution of the lengths of different-chirality s-SWCNTs. (f) Typical AFM image of high-density s-SWCNTs for the construction of thin-film transistors. (g) Statistical distribution of the densities of different-chirality s-SWCNT films for the construction of thin-film transistors. Error bars in (e) and (g) are the standard deviation of statistics. Reproduced with permission from J. Y. Ouyang *et al.*, ACS Appl. Polym. Mater. **4**, 6239–6254 (2022). Copyright 2022 American Chemical Society.

three polymers, PFO-BPy, PFO, and PFO-BT, to sort out (6,5), (7,5), and (10,5) species in the organic phase, respectively, and prepared the corresponding FETs to compare their performances. The results show that the devices prepared with large-diameter (10,5) s-SWCNTs have the best electrical properties among the three

devices, with carrier mobility up to  $16 \text{ cm}^2 \text{ V}^{-1} \text{ s}^{-1}$  and an on/off ratio of  $10^7$ . In 2021, the polymer method was used to separate (10,8) species (monochiral purity 92.3%) with large tube diameters ( $>1.24 \text{ nm}$ ), resulting in a significant improvement in the carrier mobility of the corresponding CNT FET devices. The maximum

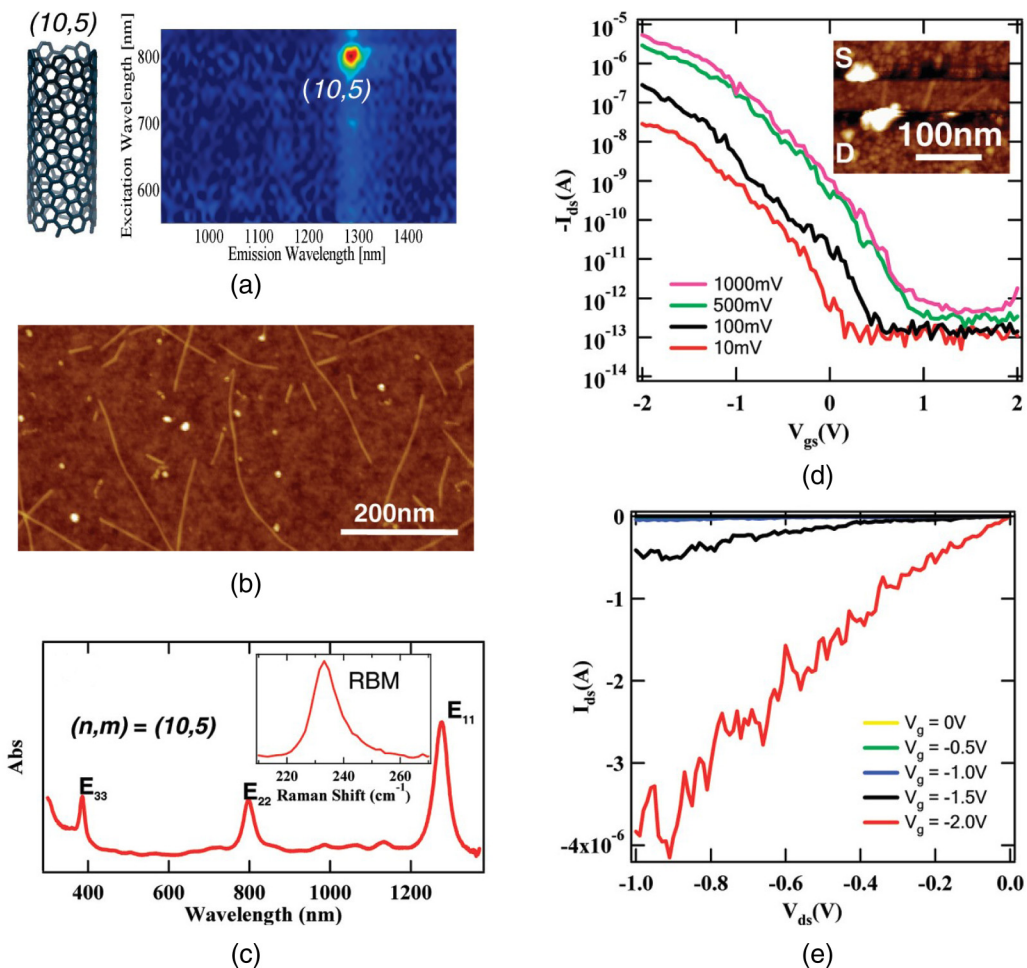


**FIG. 8.** Optical characterizations and electronic devices of nearly pure (10,5) s-SWCNTs.<sup>158</sup> (a) The photoluminescence excitation (PLE) mapping of (10,5) s-SWCNTs. (b) AFM image of the (10,5) s-SWCNTs. (c) Optical absorption spectrum of the (10,5) s-SWCNTs. Electrical transport properties of FET s-SWCNTs. (d) Transfer characteristics ( $I_{ds}$ - $V_{gs}$  curves) of a typical device made of  $\sim 15$  (10,5) s-SWCNTs at different bias voltages. (e) Current-voltage characteristics ( $I_{ds}$ - $V_{ds}$ ) of the device at different values of  $V_{gs}$ . Reproduced with permission from L. Zhang *et al.*, J. Am. Chem. Soc. **131**, 2454–2455 (2009). Copyright 2009 American Chemical Society.

23 December 2023 06:45:12

carrier mobility was  $61 \text{ cm}^2 \text{ V}^{-1} \text{ s}^{-1}$ , the average carrier mobility was  $51.6 \text{ cm}^2 \text{ V}^{-1} \text{ s}^{-1}$ , and the CNT FETs had a high switching ratio of  $10^6$ .<sup>126</sup> Green *et al.* used an orthogonal iterative DGU method for a three-step separation: (1) isolate by diameter, (2) enrich small-diameter s-SWNTs, and (3) remove metallic SWNT impurities. They obtained s-SWCNTs of nearly monochirality (6,5). The s-SWCNT FETs made from networked films of the CNTs are shown to have an on/off ratio of  $10^5$  and a carrier mobility of  $37 \text{ cm}^2 \text{ V}^{-1} \text{ s}^{-1}$ . Notably, (6,5) and (9,1) species with the same diameter of  $0.76 \text{ nm}$  were obtained by orthogonal iterative DGU. This method has now been shown to be used to separate carbon tubes of different diameters, but there is no evidence that the method is useful for separating chirality. The increase in the tube diameter is accompanied by a decrease in the bandgap and differences between chiral species, along with a greater variety of

chiralities. Peng's team at Peking University reported a method of host-guest molecular interaction between SWCNTs and inner clusters with designed size, thus selectively separating s-SWCNTs of expected diameters.<sup>157</sup> In addition, the design of polymers matched to the structure of carbon tubes is key to the chiral separation of large-tube-size s-SWCNTs.

## 2. Effect of length distribution on thin films of s-SWCNTs

In addition to the tube diameter, the length of the s-SWCNTs is one of the important factors affecting the quality of the film and the final device performance. The length and length distribution of s-SWCNTs affect the alignment process of carbon tubes. During the various separation processes for removing metal tubes, the

**TABLE II.** Advances in monochiral s-SWCNTs and corresponding CNT FETs.

Properties(Chirality		(10,8)	(12,5)	(6,5)	(7,5)	(7,6)	(7,5), (10,5)	(7,5), (10,5)	(6,5)	(9,8)	(6,5)	(6,5)	(7,5)	(10,5)
CNT Properties	SWCNT Sample	HiPco	HiPco	CoMoCat	CoMoCat	HiPco (Unidym Inc.)	Tailored (Aldrich)	CoMoCat (CHASM Advanced Materials Inc.)	CoMoCat (CHASM Advanced Materials Inc.)	CVD	HiPco (Unidym Inc.)	CoMoCAT (CHASM Advanced Materials Inc.)	CoMoCAT (CHASM Advanced Materials Inc.)	HiPco (Nanolintegris)
Processing methods for separation	Polymer wrapping PFP and PCP	Polymer wrapping PFP and PCP	Polymer wrapping PFO-BPy	ATPE	Polymer wrapping PFO	Polymer wrapping PFO	Polymer wrapping PFO and F8BT	Polymer wrapping PFO and F8BT	Polymer wrapping PFO-BPy	ATPE	Orthogonal DGU	Polymer wrapping PFO-BPy	Polymer wrapping PFO-BPy	Polymer wrapping PFO-BT
Centrifugation and duration	650000 g 6 h	650000 g 10 h	4000 rpm 0.5 h	N/A	60 000 g 45 min	60 000 g 45 min	60 000 g 45 min	60 000 g 45 min	60 000 g 60 min	100 000 g 60 min	three orthogonal DGU	70 000 g 1 h	70 000 g 1 h	70 000 g 1 h
Monochiral Purity	92.3%	95.6%	N/A	N/A	1h+20 h	1h+20 h	1h+20 h	1h+20 h	13 h	N/A	88.4% [9,1]	97%[(6,5) and (9,1)]	89.1%	79.1%
Purity	99.94%	N/A	N/A	N/A	N/A	N/A	N/A	N/A	N/A	N/A	98%	N/A	N/A	N/A
d (CNT) (nm)	1.24	1.2	0.76	0.76	0.83	0.83	0.83	0.76	0.76	0.76	0.76	0.76	0.83	N/A
Bandgap (eV)	0.8	N2A	1.27	1.27	1.211	1.211	1.211	1.27	N/A	...	1.27	1.27	1.211	1.05
$\mu$ ( $\text{cm}^2 \text{V}^{-1} \text{s}^{-1}$ )	up to 61	N/A	8.1	N/A	10	10	9	15	3.5	22.34	37	1.5	0.5	N/A
FET properties	Polarity and gate structure	Bottom	N/A	P/Bottom	N/A	Top gate	Top gate	Top gate	Top gate	P/Bottom gate	Bottom gate	Bottom gate	Bottom gate	N/A
FET Numbers	254	N/A	N/A	N/A	N/A	N/A	N/A	N/A	N/A	25	...	...	...	N/A
CNT Density (tubes / $\mu\text{m}$ )	30	N/A	N/A	N/A	9–10	8–9	3–6	≥40	50	50	...	30	30	30
$L_g W_g$ ( $\mu\text{m}$ )	0.5/10	N/A	10/500	30/NA	20/20	20/20 mm	20/20	40/1000	40/1 mm	50/200	64/250	20/400	20/400	20/400
$I_{on}$ & $I_{off}$ (A)	N/A	N/A	N/A	N/A	$10^{-4}$	$10^{-4}$	$10^{-5}$	$10^{-5}$	N/A	0.05 $\mu\text{A}/\mu\text{m}$	...	N/A	N/A	
on/off ratio	up to $10^6$	N/A	$10^4$	$10^3$	$10^6$	$10^6$	$10^6$	$10^6$	N/A	$10^{5-10^6}$	up to $10^5$	$10^{5-10^6}$	$10^{5-10^6}$	$10^7$
$V_{TH}$ (V)	N/A	N/A	-3.1	N/A	N/A	N/A	N/A	N/A	N/A	N/A	...	N/A	N/A	N/A
$V_{DS}(V)$	-1	N/A	-10	1	N/A	N/A	N/A	N/A	-0.1	0.1	...	N/A	N/A	N/A
SS (mv/dec)	178	N/A	1090	Rice	Imperial College London	University	University	Universität Heidelberg	N/A	N/A	...	N/A	N/A	N/A
Research institute	Suzhou Institute of Nano-Tech and Nano-Bionics, Chinese Academy of Sciences, China	126	131	161	151	129	162	163	79	79	79	79	79	79

length of carbon nanotubes is truncated due to a number of physical and chemical methods, resulting in a large number of short carbon tubes. When prepared as thin films, the shorter average tube length leads to an increase in the number of laps between carbon nanotubes, thus prolonging the carrier transport path and increasing the chance of carrier scattering. This ultimately leads to a decrease in the carrier mobility of the device, which severely restricts the development of high-performance s-SWCNT FETs. Li Qingwen *et al.* separated high-purity s-SWCNT solutions with polymer PCz. After the cyclic deposition process, the content of short carbon tubes in the dispersion was drastically reduced and the average length of s-SWCNTs was improved. The s-SWCNT FETs prepared from long carbon nanotubes have excellent electrical performance with an on/off ratio of  $10^7$  and a carrier mobility of  $34 \text{ cm}^2 \text{ V}^{-1} \text{ s}^{-1}$ , which is a threefold improvement over the electrical performance of the corresponding s-SWCNT FETs prepared from short tubes.<sup>159,160</sup> Therefore, optimizing the length distribution of monochiral s-SWCNTs is an effective solution to improve the electrical properties of s-SWCNT FETs. Table II summarizes the s-SWCNT FETs prepared from monochiral s-SWCNT isolated from polyfluorene and its derivatives.

In order to isolate high-purity monochiral s-SWCNTs, optimization is required in terms of diameter and length distribution of raw materials, polymer type, polymer to CNT ratio, solution selection, temperature, and centrifugation parameters. The preparation of "high-quality" s-SWCNT films requires high-purity,<sup>126,164,165</sup> nearly monochiral,<sup>126,129,164,165</sup> large tube diameters ( $>1.2 \text{ nm}$ ),<sup>151,166,167</sup> and uniformly arranged,<sup>121,140,161,168</sup> s-SWCNTs. Due to the smaller bandgap of large-diameter s-SWCNTs,<sup>129,151,166,167</sup> the carriers are preferentially transported in the large-diameter carbon tubes. When the carbon tube density of the s-SWCNT film increases, more s-SWCNTs participate in the current transport at the same time.<sup>106,126,162</sup> The interaction of nanoscaled objects such as s-SWCNTs with a surface can lead to substantial binding energies of 0.8. As a consequence, nanotubes tend to distort so as to conform to the topography of the substrate.<sup>169</sup> This distortion may cause an increase in the number of overlapping times between carbon nanotubes, which can have implications for the electrical properties of nanotubes. The homogeneous array reduces the overlap of different carbon tubes and decreases the negative effect of inter-tube contact resistance.<sup>151</sup> Therefore, high-purity, nearly monochiral, large tube diameter ( $>1.2 \text{ nm}$ ), high-density, and uniformly arranged s-SWCNTs are the material basis for high-performance s-SWCNT FETs.<sup>20,100,116,121,152</sup>

### C. Other factors to optimize s-SWCNT FETs

In order to obtain high-performance s-SWCNT FETs, it is necessary to prepare "high-quality" s-SWCNT films on the one hand and refer to the optimization of Si-based FETs on the other. For example, the effects of the gate structure,<sup>126,143</sup> channel width,<sup>126</sup> and electrode material on the performance of s-SWCNT FETs should be considered. (1) Gate structure. The main gate geometries are back gate, top gate, double gate, and gate-all-around. High-performance s-SWCNT FETs are mostly top-gate structures due to their high gate capacitance and gate control capability.

Researchers have innovated in the gate structure. Liu *et al.* fabricated and characterized a TiN floating-gate dual-gate device that utilizes a CNT network as the channel material.<sup>173</sup> By modulating the conducting state in the CNT channel with the charge stored in the floating gate, they can control the device state on the top side flexibly. This means the information stored in the floating gate can be used as an input signal in the top-gate device for logic computing. The gate pitch (CGP) is one of the most important metrics to measure IC integration. In 2023, Peng's research group prepared CNT FETs based on arrayed CNTs with an on-state current (Ion) of  $2.24 \text{ mA}/\mu\text{m}$  and a peak transconductance (gm) of  $1.64 \text{ mS}/\mu\text{m}$ . The CNT FETs were integrated into a static random-access memory cell with an area of  $0.976 \mu\text{m}^2$ , comparable to a 90 nm silicon technology node. These results demonstrate the potential of arrayed CNT FETs for high-performance ICs at the 10 nm node, offering the possibility of integration enhancement for carbon-based ICs. (2) Channel width. Li *et al.* showed that as the channel width of CNT FETs decreases, the on-state current density increases. The on-state current density increases by 300% for 300 nm channel width compared to CNT FETs with 500 nm channel width.<sup>126</sup> (3) Electrode material. For quasi-ballistic transport CNT FETs, when the channel length is smaller than the CNT mean free range, the contact resistance occupies almost all of the device resistance. Therefore, on the one hand, while optimizing the materials and device process to obtain high carrier mobility, the contact resistance needs to be as small as possible for a given electrode size. The selection of electrode materials is also a key concern for researchers. Earlier studies confirmed that the contact barriers are large when Pt and Au are used as electrodes. In 2003, Javey *et al.* found that when palladium (Pd) is used as the electrode material, the prepared CNT FETs can realize P-type ohmic contacts with open-state conductance close to the theoretical limit of quantum conductance at room temperature. However, there have been many difficulties in the preparation of high-performance N-type carbon nanotubes. In 2007, Peng's group prepared the first N-type CNT-based complementary metal-oxide semiconductor using Sc electrodes.<sup>174</sup> In 2022, their array CNT-based N-type CNT FETs achieved an Ion of  $800 \mu\text{A}/\mu\text{m}$  and a gm of  $250 \mu\text{S}/\mu\text{m}$ , representing the highest performance of CNT-based N-FETs to date.<sup>175</sup> The performance of short channel n-type FETs is improved here by using scandium contacts accompanied by a doping channel and high-performance and symmetrical CMOS FETs with a deep sub-micrometer gate length are fabricated for the first time.<sup>176</sup> In Fig. 9, the characterization of some species and common device structures are shown.

### D. RF applications for CNT FETs

Recently, radio frequency (RF) devices have received increasing attention. The next generation of wireless communications requires RF devices that can operate at frequencies greater than 90 GHz. Silicon transistors are capable of high levels of integration at low cost, but they suffer from poor linearity and noise performance at frequencies above 20 GHz.<sup>158,177</sup> III–IV compound semiconductor-based RF devices have good performance, but their processes are complex and less integrated. Both of them are difficult to meet the needs of the RF electronics field. With high carrier

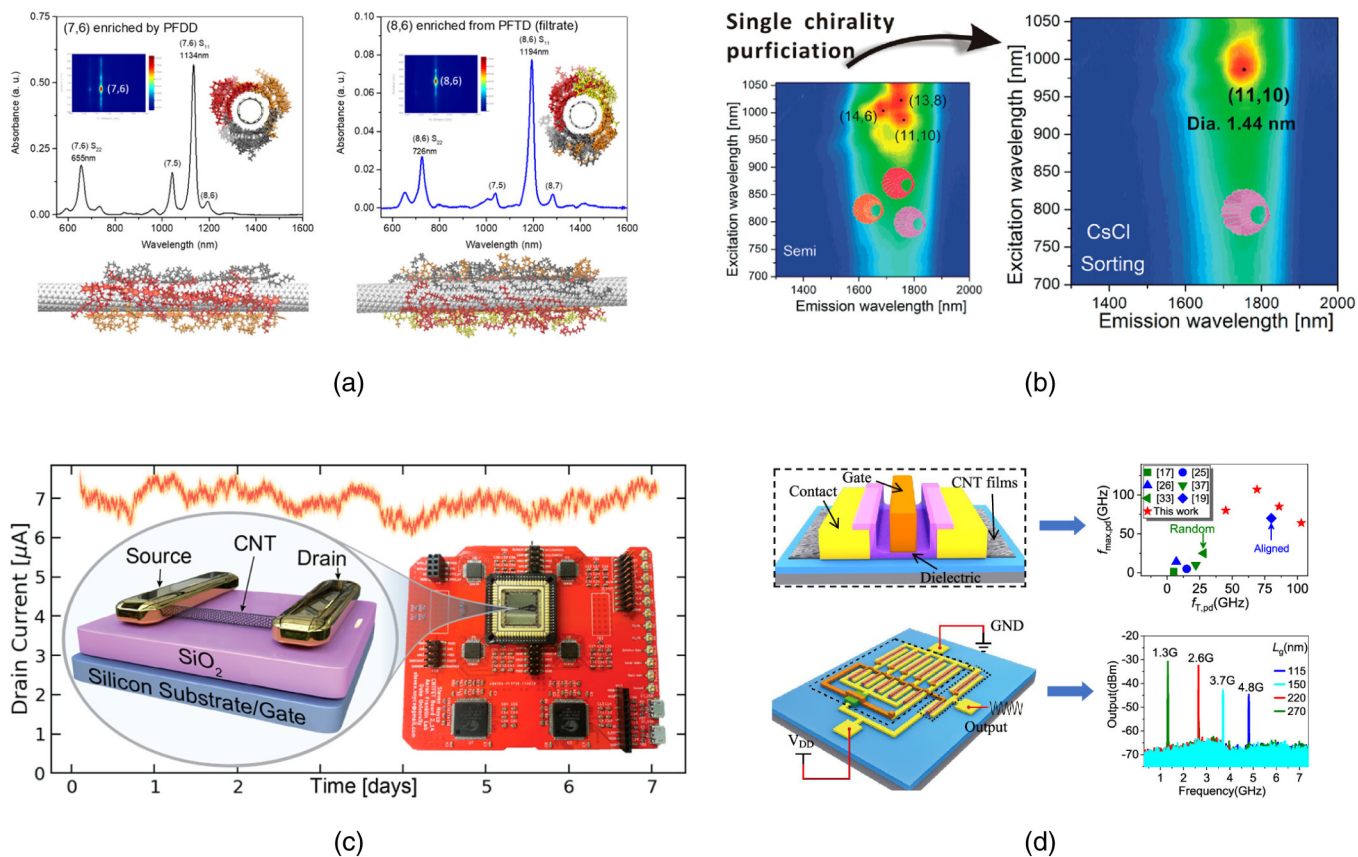


**FIG. 9.** (a) Optimal binding geometries of polymers on the surface of (7,6) and (8,6) nanotubes.<sup>113</sup> Reproduced with permission from J. Ouyang *et al.*, ACS Appl. Polym. Mater. **4**, 6239–6254 (2022). Copyright 2022 American Chemical Society. (b) PLE mapping of (*n,m*) monochirality SWCNTs.<sup>170</sup> Reproduced with permission from M. Kawai *et al.*, J. Am. Chem. Soc. **134**, 9545–9548 (2012). Copyright 2012 American Chemical Society. (c) CNT FET schematic with Pd source/drain contacts, 90 nm SiO<sub>2</sub> gate dielectric, and photo of fully automated PCB measurement platform: stand-alone, wireless, and programmable.<sup>171</sup> Reproduced with permission from S. G. Noyce *et al.*, Nano Lett. **19**, 1460–1466 (2019). Copyright 2019 American Chemical Society. (d) Schematic of a CNT RF transistor with Ground-Signal-Ground (GSG) pads. Inset: structure of the channel region. The air gaps help suppress the parasitic capacitance.<sup>172</sup> Reproduced with permission from L. Zhang *et al.*, J. Am. Chem. Soc. **131**, 2454–2455 (2009). Copyright 2009 American Chemical Society.

23 December 2023 06:45:12

mobility, small intrinsic capacitance, high thermal stability, and thermal conductivity, CNTs have the advantage of preparing FETs with high operating frequency.<sup>177,178</sup> RF CNT FETs are one of the most promising devices beyond RF CMOS technology. However, the actual values of some performance indexes of RF CNT FETs, such as current gain cut-off frequency ( $f_T$ ), power gain cut-off frequency ( $f_{MAX}$ ), and transconductance ( $g_m$ ), are lower than the theoretical values. The improvement of the performance of RF CNT FETs requires further optimization of material properties and device structure. Tables III and IV summarize the research progress of RF CNT FETs, and readers can get detailed information from the table.

Table III summarizes the RF CNT FETs prepared from s-SWCNT networked films. Low-purity networked or partially oriented s-SWCNTs films were prepared by dielectrophoresis, and RF CNT FETs with a back-gate structure were prepared with this film. However, the performance of RF CNT FETs is far from the

ideal value.<sup>177</sup> The high-purity s-SWCNTs can provide large open-state currents, and the optimized device structure such as the T-gate can reduce the parasitic resistance and parasitic capacitance, so the performance indexes of RF CNT FETs, such as  $f_T$ ,  $f_{MAX}$ , and  $g_m$ , can be improved,<sup>172,181–185</sup> as shown in Table III. However, the random orientation of the network film leads to a random distribution of the carbon tube lengths in the channel, which increases the gate capacitance and decreases the  $g_m$ .<sup>177</sup> Therefore, the uniformly aligned s-SWCNTs are more suitable for RF CNT FET applications. RF CNT FETs prepared from arrays of s-SWCNTs are summarized in Table IV. Compared with the electrophoretic method, the s-SWCNT arrays grown by the CVD method realized the performance enhancement simply by improving the arrangement of carbon tubes.<sup>187,192</sup> However, the CVD method cannot avoid metal tube residues, and the selective etching of metal tubes brings negative effects such as carrier mobility decrease and parasitic capacitance increase. With the

TABLE III. Advances in RF CNT FETs prepared from network thin films.

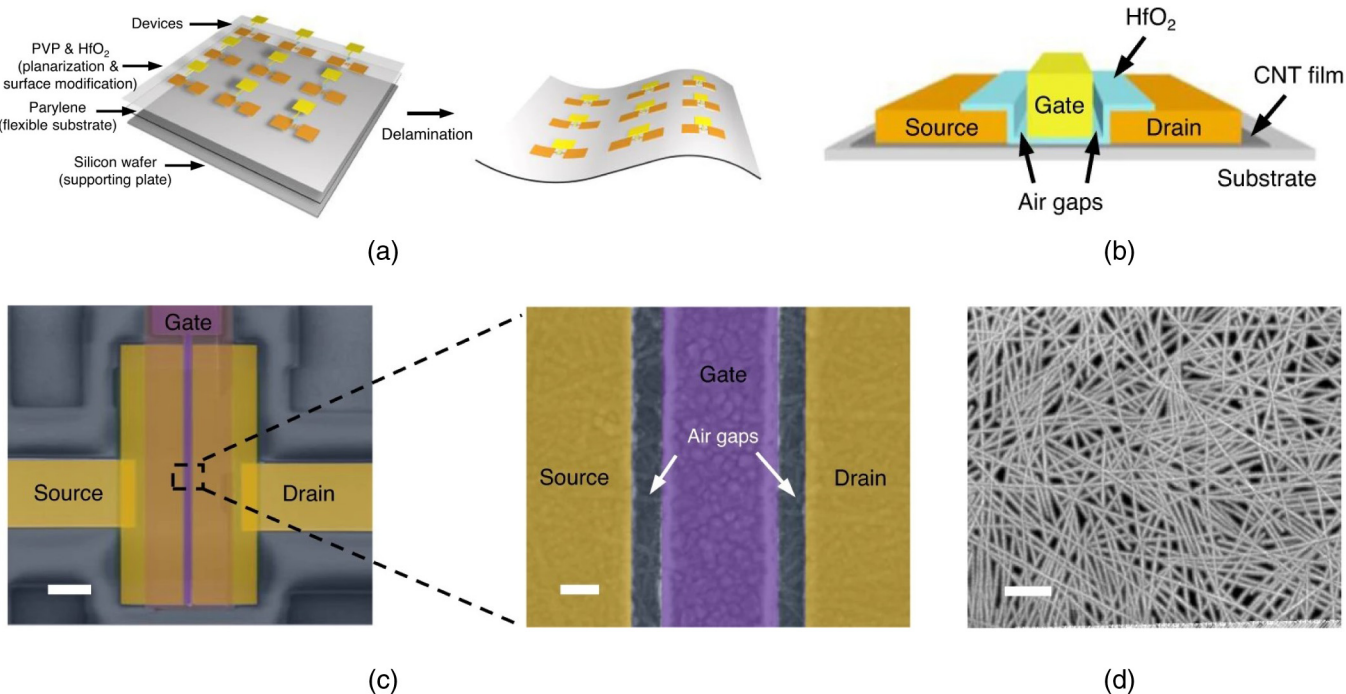
Properties\Year		2006 <sup>179</sup>	2007 <sup>180</sup>	2009 <sup>181</sup>	2012 <sup>182</sup>	2015 <sup>183</sup>	2016 <sup>184</sup>	2019 <sup>172</sup>	2021 <sup>185</sup>
CNT properties	Processing methods for separation Purity (semiconductor)	dielectrophoresis	Dielectrophoresis	Dielectrophoresis	...	Polymer wrapping >99.99%	>99%	...	Polymer wrapping >99.99%
RF-FET properties	d (CNT) (nm)	...	...	99%	98%	...	1.6	1.5	...
	arrangement Network	...	Oriented	Network	Network	Network	...	Network	Network
	$\mu$ ( $\text{cm}^2 \text{V}^{-1} \text{s}^{-1}$ )	...	...	...	...	...	...	...	...
	Gate structure	Back gate	Back gate	Back gate	T-gate	T-gate	...	Top gate	Top gate
	$g_m$	$500 \mu\text{S}$	$500 \mu\text{S}$	$2.66 \text{ mS}$	$40 \mu\text{S}/\mu\text{m}$	$55 \mu\text{S}/\mu\text{m}$	$380 \mu\text{S}/\mu\text{m}$	$520 \mu\text{S}/\mu\text{m}$	$520 \mu\text{S}/\mu\text{m}$
	CNT density (tubes / $\mu\text{m}$ )	10	>10	...	...	10	50	50	60
	$L_g W_g$	300 nm/10 $\mu\text{m}$	300 nm/10 $\mu\text{m}$	300 nm/10 $\mu\text{m}$	140 nm/50 $\mu\text{m}$	120 nm/30 $\mu\text{m}$	120 nm/50 $\mu\text{m}$	130 nm/90 $\mu\text{m}$	80 nm/–
Electrode material and thicknesses	Pa/Au 10 $\mu\text{m}/$ 150 $\mu\text{m}$	...	...	...	...	...	Ti/Au/Pa 1 mm/50 nm/	Pd/Au 10 nm/mm/20 nm	Pd/Au 10 nm/20 nm
Research institute	Institut d'Electronique, de Microelectronique et de Nanotechnologie	University of Southern California	Peking University, China	Peking University, China					

TABLE IV. Advances in RF CNT FETs prepared from array thin films.

Properties/Year	2007 <sup>186</sup>	2009 <sup>187</sup>	2012 <sup>188</sup>	2013 <sup>189</sup>	2016 <sup>190</sup>	2019 <sup>191</sup>	2021 <sup>158</sup>
CNT properties	Processing methods for separation	CVD	Dielectrophoresis	CVD	Polymer wrapping dose-controlled, floating evaporative self-assembly method (DFES)	Polymer wrapping ZEBRA	Polymer wrapping
RF-FET properties	Purity (semiconductor) $d$ (CNT) (nm) arrangement $\mu$ ( $\text{cm}^2 \text{V}^{-1} \text{s}^{-1}$ ) Gate structure $g_m$ CNT density (tubes / $\mu\text{m}$ ) $L_g/W_g$	... ... Array ... Double gate ... 10	... ... Array ... Buried gate 5 mS 2-5	99.6% 1.5 Array ... T-gate 15 $\mu\text{S}/\mu\text{m}$ 5	... ... Array ... T-gate 310 $\mu\text{S}/\mu\text{m}$ 40	... ... Array ... T-gate 40-60	>99.9% 1.51 $\pm$ 0.18 Array 1580 Top gate 1400 $\mu\text{S}/\mu\text{m}$ 100-120
Electrode material and thicknesses	5 $\mu\text{m}/$ 200 $\mu\text{m}$ Ti/Pd 1 nm/20 nm	700 nm/ 100 $\mu\text{m}$	100 nm/-	100 nm/-	-10 $\mu\text{m}$	110 nm/25 $\mu\text{m}$	50 nm/
Research institute	University of Illinois at Urbana Champaign	J. Watson Research Center	IBM Thomas J. Watson Research Center	University of Southern California	Institut d'Electronique de Microelectronique et de Nanotechnologie	Carbonics Inc., Culver City, CA, USA	Peking University, China

TABLE V. Research Progress on Flexible CNT FETs.

Properties\Year		2020 <sup>204</sup>	2020 <sup>205</sup>	2021 <sup>206</sup>	2022 <sup>207</sup>	2022 <sup>208</sup>	2022 <sup>209</sup>	2022 <sup>210</sup>	2023 <sup>210</sup>
CNT properties	Processing methods for separation	...	Polymer wrapping	...	Polymer wrapping	...	Oxygen-assisted floating catalyst CVD	Polymer wrapping	Polymer wrapping
	Purity (semiconductor)	99%	...	...	...	...	96%	...	...
	d (CNT) (nm)	...	...	...	...	...	...	...	...
	arrangement	Network	...	Array	Network	...	1.1	1.9–2.3	...
	$\mu$ ( $\text{cm}^2 \text{V}^{-1} \text{s}^{-1}$ )	5	22.7	12.6	64.2	...	...	...	...
Substrate/thicknesses	Kapton/127 $\mu\text{m}$	Poly(ethylene naphthalate)/125 $\mu\text{m}$	Poly(ethylene terephthalate)/125 $\mu\text{m}$	Parylene/2 $\mu\text{m}$	Poly(ethylene naphthalate)/125 $\mu\text{m}$	496	35.4	11.9	Polyethylene terephthalate
FET properties	Gate structure	Top gate	Floating gate	Top gate	...	...	Back gate	Back gate	Top gate
	$g_{\text{on}}$ ( $\mu\text{S} \mu\text{m}^{-2}$ )	...	...	...	123.3	...	...	...	...
	$I_{\text{on}}$ ( $\mu\text{A} \mu\text{m}^{-2}$ )	...	...	...	187.6	...	...	...	...
	CNT Density (tubes/ $\mu\text{m}$ )	...	...	...	60	...	...	...	60
	$L_{\text{ch}}$	500 $\mu\text{m}$	...	100 $\mu\text{m}$	450 nm	...	100 $\mu\text{m}$	100 $\mu\text{m}$	110 $\mu\text{m}$
	Electrode material and thicknesses	Ag	Ti/Au 5 nm/50 nm	Ag	Pa/Au 60 nm/20 nm	Ti/Au 10 nm/100 nm	Ti/Au 10 nm/100 nm	Ti/Au 10 nm/100 nm	Ag
	$I_{\text{on}}/I_{\text{off}}$ ratio	$10^5$	$10^6$	$10^5$	$10^4$	$10^8$	$10^6$	$10^6$	$\pm 1$
	$V_{\text{GS}}$ (V)	$\pm 10$	0	$\pm 1$	...	...	...	...	...
	$V_{\text{DS}}$ (V)	...	1	...	-0.1	-0.5	...	...	...
	SS (mv dec $^{-1}$ )	...	140	70	...	...	...	...	70–80
Research institute	School of Electrical and Computer Engineering, Georgia Institute of Technology, Atlanta 30332, GA, United States of America	Shenyang National Laboratory for Materials Science, Institute of Engineering Science and Nanodevices, School of Electronics and Nanoscience, Shenyang National Laboratory for Materials Science, Institute of Metal Research Chinese Academy of Sciences, China	Key Laboratory for the Physics and Chemistry of Nanodevices, School of Materials Science and Engineering Zhengzhou University, China	Shenyang National Laboratory for Materials Science, Institute of Metal Research Chinese Academy of Sciences, China	Institute of Nano Science and Technology, University of Science and Technology of China, China				



**FIG. 10.** (a) Schematic illustration of device and circuit fabrication on a flexible parylene substrate. (b) Schematic diagram of a flexible CNT TFT. (c) False-colored SEM image of a TFT with a channel length of 450 nm. Scale bar, 2  $\mu$ m. (d) Magnified SEM image of the channel region of the device, scale bar, 100 nm. (e) SEM image of the randomly oriented CNT network in the channel. Scale bar, 200 nm.<sup>211</sup> Reproduced with permission from G. H. Long *et al.*, Nat. Commun. **13**, 6734 (2022). Copyright 2022 Springer Nature.

23 December 2023 06:45:12

development of separation methods, high semiconductor purity, uniformly aligned s-SWCNTs can be prepared, and combined with the optimization of the device structure,<sup>158,188–191</sup> the carbon-based RF devices have a great potential for applications in the terahertz band.<sup>158</sup> However, the yield and purity of the separation of monochiral s-SWCNTs are low, and there are many problems to be overcome in the preparation of monochiral s-SWCNT films. It has been demonstrated that network thin films of monochiral s-SWCNTs can be successfully prepared, such as Liu *et al.* developed the alkaline small molecule regulation technique based on the traditional deposition method.<sup>35,152</sup> Before deposition, NaHCO<sub>3</sub> was introduced into the solution to enhance the interaction between s-SWCNTs and functionalized substrates. The substrate was then immersed into poly-L-lysine (PLL) aqueous solution to achieve amine functionalization. Next, the amine functionalized substrates were immersed into the as-prepared monochirality SWCNT solution for 1 h to prepare films. However, the network films prepared by this method still suffer from the problem of low density, and hence, the performance index of the corresponding CNT FETs needs to be improved. In addition, the preparation of monochiral s-SWCNT network films is only the first step to utilize the great material advantages of the monochiral s-SWCNT. How to improve the yield and purity of the monochiral s-SWCNT and prepare high-purity uniformly aligned monochiral s-SWCNT arrays is the ultimate goal of the researchers.

## E. Flexible electronics applications for CNT FETs

In recent years, flexible electronics have attracted great interest, including flexible displays,<sup>193,194</sup> wearable devices,<sup>195,196</sup> and implantable medical devices.<sup>197,198</sup> High-performance ICs, as the core unit of flexible electronics, need to have both good electrical properties and mechanical flexibility, and be able to be integrated with other components. Conventional silicon-based technologies involve high-temperature doping processes that are incompatible with the plastic substrates used in flexible electronics.<sup>199</sup> s-SWCNTs are one of the most promising materials in the field of flexible electronics due to their excellent electrical properties, mechanical flexibility, and stretchability.<sup>200–203</sup> The advantages of s-SWCNTs on traditional rigid substrates can be extended to flexible substrates by choosing suitable flexible substrate materials<sup>164,165</sup> such as polyimide foils.<sup>131</sup> Table V summarizes recent research progress in flexible CNT FETs. Peng's research group designed CNT TFTs with a channel length of 450 nm on a 2  $\mu$ m-thick poly(parylene) substrate, as shown in Fig. 10. Its on-state current is  $187.6 \mu\text{A} \mu\text{m}^{-1}$  and transconductance is  $123.3 \mu\text{S} \mu\text{m}^{-1}$ ,<sup>211</sup> which are comparable to the rigid device. Despite the great potential of s-SWCNTs in flexible electronics, CNT FETs still suffer from problems such as the stability of electrical properties. This problem can be improved by using monochiral s-SWCNTs with homogeneous properties to act as channel materials. Michael *et al.* used bilayer

graphene-s-SWCNT (12,6) hybrid films as channel materials for flexible CNT FETs, solving the problem of high contact resistance of s-SWCNTs and obtaining ideal electrical conductivity.<sup>212</sup> Overall, there are fewer reports on the preparation of flexible CNT FETs with monochiral s-SWCNTs, and there is still a long way to go for the application of monochiral s-SWCNTs in the field of flexible electronics.<sup>211</sup>

## IV. CONCLUSIONS AND FUTURE OUTLOOK

The superiority of s-SWCNTs as a next-generation electronic material that may replace silicon has been well proven. Compared to s-SWCNTs, monochiral s-SWCNTs have great potential for the development of high-end ICs. However, efforts from the following two aspects are still needed before they can realize industrial applications. (1) Further development of controlled growth or post-processing purification techniques is needed to obtain low-cost, high-yield, high-purity monochiral s-SWCNTs. In addition, the film-making process is optimized to obtain high-quality monochiral s-SWCNTs array films. (2) By optimizing the device structure and preparation process of CNT FETs, the material intrinsic advantages of CNTs can be fully utilized to realize high-speed, low-power CNT ICs, providing a possible solution for the post-Moore era.

## ACKNOWLEDGMENTS

This work was financially supported by the National Natural Science Foundation of China (Grant No. 62274130), the Fundamental Research Funds for the Central Universities (Grant No. QTZX22063), the Fund from the Department of Science and Technology in Shaanxi Province (Grant No. 2016FWPT-09), the Natural Science Basic Research Plan of Shaanxi Province (Grant No. 2022JM-088), the National Natural Science Foundation of China (Grant No. 62188102), and the Joint Fund of the Ministry of Education (Grant No. 8091B042112).

## AUTHOR DECLARATIONS

### Conflict of Interest

The authors have no conflicts to disclose.

### Author Contributions

Yanan Sun and Jiejie Zhu contributed equally to the article.

**Yanan Sun:** Conceptualization (equal); Investigation (equal); Writing – original draft (equal). **Jiejie Zhu:** Investigation (equal); Validation (equal); Writing – original draft (equal). **Wenhui Yi:** Investigation (equal); Validation (equal). **Yuxiang Wei:** Investigation (equal); Validation (equal). **Xuejiao Zhou:** Investigation (supporting). **Peng Zhang:** Investigation (supporting). **Yang Liu:** Investigation (supporting). **Peixian Li:** Investigation (supporting). **Yimin Lei:** Funding acquisition (equal); Investigation (equal); Writing – original draft (equal); Writing – review & editing (equal). **Xiaohua Ma:** Funding acquisition (equal); Validation (equal); Writing – review & editing (equal).

## DATA AVAILABILITY

The data that support the findings of this study are available from the corresponding authors upon reasonable request.

## REFERENCES

- <sup>1</sup>A. S. R. Bati, L. P. Yu *et al.*, “Recent advances in applications of sorted single-walled carbon nanotubes,” *Adv. Funct. Mater.* **29**, 1902273 (2019).
- <sup>2</sup>Z. D. Han and A. Fina, “Thermal conductivity of carbon nanotubes and their polymer nanocomposites: A review,” *Prog. Polym. Sci.* **36**, 914–944 (2011).
- <sup>3</sup>D. Janas, “Towards monochiral carbon nanotubes: A review of progress in the sorting of single-walled carbon nanotubes,” *Mater. Chem. Front.* **2**, 36–63 (2018).
- <sup>4</sup>R. Rao, C. L. Pint *et al.*, “Carbon nanotubes and related nanomaterials: Critical advances and challenges for synthesis toward mainstream commercial applications,” *ACS Nano* **12**, 11756–11784 (2018).
- <sup>5</sup>W. A. G. Rojas and M. C. Hersam, “Chirality-enriched carbon nanotubes for next-generation computing,” *Adv. Mater.* **32**, 1905654 (2020).
- <sup>6</sup>N. Tessler, Y. Preezant *et al.*, “Charge transport in disordered organic materials and its relevance to thin-film devices: A tutorial review,” *Adv. Mater.* **21**, 2741–2761 (2009).
- <sup>7</sup>B. L. Liu, F. Q. Wu *et al.*, “Chirality-controlled synthesis and applications of single-wall carbon nanotubes,” *ACS Nano* **11**, 31–53 (2017).
- <sup>8</sup>S. Park, M. Vosguerichian *et al.*, “A review of fabrication and applications of carbon nanotube film-based flexible electronics,” *Nanoscale* **5**, 1727–1752 (2013).
- <sup>9</sup>S. Qiu, K. J. Wu *et al.*, “Solution-processing of high-purity semiconducting single-walled carbon nanotubes for electronics devices,” *Adv. Mater.* **31**, 2122 (2019).
- <sup>10</sup>T. Durkop, S. A. Getty *et al.*, “Extraordinary mobility in semiconducting carbon nanotubes,” *Nano Lett.* **4**, 35–39 (2004).
- <sup>11</sup>S. Talapatra, S. Kar *et al.*, “Direct growth of aligned carbon nanotubes on bulk metals,” *Nat. Nanotechnol.* **1**, 112–116 (2006).
- <sup>12</sup>M. V. Kharlamova, M. G. Burdanova *et al.*, “Synthesis, sorting, and applications of single-chirality single-walled carbon nanotubes,” *Materials* **15**, 44 (2022).
- <sup>13</sup>X. J. Wei, S. L. Li *et al.*, “Recent advances in structure separation of single-wall carbon nanotubes and their application in optics, electronics, and optoelectronics,” *Adv. Sci.* **9**, 2200054 (2022).
- <sup>14</sup>R. H. Baughman, A. A. Zakhidov *et al.*, “Carbon nanotubes—The route toward applications,” *Science* **297**, 787–792 (2002).
- <sup>15</sup>M. F. L. De Volder, S. H. Tawfick *et al.*, “Carbon nanotubes: Present and future commercial applications,” *Science* **339**, 535–539 (2013).
- <sup>16</sup>J.-P. Salvetat, J.-M. Bonard *et al.*, “Physical properties of carbon nanotubes,” *AIP Conf. Proc.* **442**, 467–480 (1998).
- <sup>17</sup>J. W. G. Wildoer, L. C. Venema *et al.*, “Electronic structure of atomically resolved carbon nanotubes,” *Nature* **391**, 59–62 (1998).
- <sup>18</sup>J. Y. Wang and T. Lei, “Separation of semiconducting carbon nanotubes using conjugated polymer wrapping,” *Polymers* **12**, 1548 (2020).
- <sup>19</sup>G. G. Samsonidze, R. Saito *et al.*, “Family behavior of the optical transition energies in single-wall carbon nanotubes of smaller diameters,” *Appl. Phys. Lett.* **85**, 5703–5705 (2004).
- <sup>20</sup>G. J. Brady, A. J. Way *et al.*, “Quasi-ballistic carbon nanotube array transistors with current density exceeding Si and GaAs,” *Sci. Adv.* **2**, e1601240 (2016).
- <sup>21</sup>S. Hong and S. Myung, “Nanotube electronics—A flexible approach to mobility,” *Nat. Nanotechnol.* **2**, 207–208 (2007).
- <sup>22</sup>D. Janas, A. P. Herman *et al.*, “Iodine monochloride as a powerful enhancer of electrical conductivity of carbon nanotube wires,” *Carbon* **73**, 225–233 (2014).
- <sup>23</sup>L. P. Yu, C. Shearer *et al.*, “Recent development of carbon nanotube transparent conductive films,” *Chem. Rev.* **116**, 13413–13453 (2016).
- <sup>24</sup>D. Janas, N. Czechowski *et al.*, “Electroluminescence from carbon nanotube films resistively heated in air,” *Appl. Phys. Lett.* **102**, 181104 (2013).

- <sup>25</sup>H. Kataura, Y. Kumazawa *et al.*, "Optical properties of single-wall carbon nanotubes," *Synth. Met.* **103**, 2555–2558 (1999).
- <sup>26</sup>A. Star, Y. Lu *et al.*, "Nanotube optoelectronic memory devices," *Nano Lett.* **4**, 1587–1591 (2004).
- <sup>27</sup>K. K. Koziol, D. Janas *et al.*, "Thermal properties of continuously spun carbon nanotube fibres," *Phys. E: Low-Dimens. Syst. Nanostruct.* **88**, 104–108 (2017).
- <sup>28</sup>E. Pop, D. Mann *et al.*, "Thermal conductance of an individual single-wall carbon nanotube above room temperature," *Nano Lett.* **6**, 96–100 (2006).
- <sup>29</sup>D. Janas, N. Czechowski *et al.*, "Direct evidence of delayed electroluminescence from carbon nanotubes on the macroscale," *Appl. Phys. Lett.* **104**, 261107 (2014).
- <sup>30</sup>W. Zhang, Z. Y. Zhu *et al.*, "Chirality dependence of the thermal conductivity of carbon nanotubes," *Nanotechnology* **15**, 936–939 (2004).
- <sup>31</sup>M. F. Yu, B. S. Files *et al.*, "Tensile loading of ropes of single wall carbon nanotubes and their mechanical properties," *Phys. Rev. Lett.* **84**, 5552–5555 (2000).
- <sup>32</sup>M. F. Yu, O. Lourie *et al.*, "Strength and breaking mechanism of multiwalled carbon nanotubes under tensile load," *Science* **287**, 637–640, (2000).
- <sup>33</sup>B. I. Yakobson, C. J. Brabec *et al.*, "Nanomechanics of carbon tubes: Instabilities beyond linear response," *Phys. Rev. Lett.* **76**, 2511–2514 (1996).
- <sup>34</sup>B. I. Yakobson, G. Samsonidze *et al.*, "Atomistic theory of mechanical relaxation in fullerene nanotubes," *Carbon* **38**, 1675–1680 (2000).
- <sup>35</sup>W. Su, X. Li *et al.*, "Chirality-dependent electrical transport properties of carbon nanotubes obtained by experimental measurement," *Nat. Commun.* **14**, 1672 (2023).
- <sup>36</sup>S. Liang, N. Wei *et al.*, "Microcavity-controlled chirality-sorted carbon nanotube film infrared light emitters," *ACS Photonics* **4**, 435–442 (2017).
- <sup>37</sup>M. C. Hersam, "Progress towards monodisperse single-walled carbon nanotubes," *Nat. Nanotechnol.* **3**, 387–394 (2008).
- <sup>38</sup>R. Arenal, P. Lothman *et al.*, "Direct evidence of atomic structure conservation along ultra-long carbon nanotubes," *J. Phys. Chem. C* **116**, 14103–14107 (2012).
- <sup>39</sup>Y. C. Che, C. Wang *et al.*, "Selective synthesis and device applications of semiconducting single-walled carbon nanotubes using isopropyl alcohol as feedstock," *ACS Nano* **6**, 7454–7462 (2012).
- <sup>40</sup>G. Lolli, L. A. Zhang *et al.*, "Tailoring (n,m) structure of single-walled carbon nanotubes by modifying reaction conditions and the nature of the support of CoMo catalysts," *J. Phys. Chem. B* **110**, 2108–2115 (2006).
- <sup>41</sup>M. Fouquet, B. C. Bayer *et al.*, "Highly chiral-selective growth of single-walled carbon nanotubes with a simple monometallic Co catalyst," *Phys. Rev. B* **85**, 235411 (2012).
- <sup>42</sup>S. M. Bachilo, L. Balzano *et al.*, "Narrow (n,m)-distribution of single-walled carbon nanotubes grown using a solid supported catalyst," *J. Am. Chem. Soc.* **125**, 11186–11187 (2003).
- <sup>43</sup>F. Yang, X. Wang *et al.*, "Growing zigzag (16,0) carbon nanotubes with structure-defined catalysts," *J. Am. Chem. Soc.* **137**, 8688–8691 (2015).
- <sup>44</sup>B. L. Liu, J. Liu *et al.*, "Nearly exclusive growth of small diameter semiconducting single-wall carbon nanotubes from organic chemistry synthetic end-cap molecules," *Nano Lett.* **15**, 586–595 (2015).
- <sup>45</sup>D. W. Lin, S. C. Zhang *et al.*, "Microwave-assisted regeneration of single-walled carbon nanotubes from carbon fragments," *Small* **14**, 1800033 (2018).
- <sup>46</sup>F. Yang, X. Wang *et al.*, "Chirality-specific growth of single-walled carbon nanotubes on solid alloy catalysts," *Nature* **510**, 522–524 (2014).
- <sup>47</sup>R. E. Smalley, Y. B. Li *et al.*, "Single wall carbon nanotube amplification: En route to a type-specific growth mechanism," *J. Am. Chem. Soc.* **128**, 15824–15829 (2006).
- <sup>48</sup>Y. G. Yao, C. Q. Feng *et al.*, "Cloning' of single-walled carbon nanotubes via open-end growth mechanism," *Nano Lett.* **9**, 1673–1677 (2009).
- <sup>49</sup>M. S. He, S. C. Zhang *et al.*, "Designing catalysts for chirality-selective synthesis of single-walled carbon nanotubes: Past success and future opportunity," *Adv. Mater.* **31**, 1800805 (2019).
- <sup>50</sup>J. T. Wang, X. Jin *et al.*, "Growing highly pure semiconducting carbon nanotubes by electrotwisting the helicity," *Nat. Catal.* **1**, 326–331 (2018).
- <sup>51</sup>Q. R. Wu, L. Qiu *et al.*, "Temperature-dependent selective nucleation of single-walled carbon nanotubes from stabilized catalyst nanoparticles," *Chem. Eng. J.* **431**, 133487 (2022).
- <sup>52</sup>G. Hong, Y. B. Chen *et al.*, "Controlling the growth of single-walled carbon nanotubes on surfaces using metal and non-metal catalysts," *Carbon* **50**, 2067–2082 (2012).
- <sup>53</sup>B. L. Liu, W. C. Ren *et al.*, "Manganese-catalyzed surface growth of single-walled carbon nanotubes with high efficiency," *J. Phys. Chem. C* **112**, 19231–19235 (2008).
- <sup>54</sup>D. Takagi, Y. Homma *et al.*, "Single-walled carbon nanotube growth from highly activated metal nanoparticles," *Nano Lett.* **6**, 2642–2645 (2006).
- <sup>55</sup>Z. Zhu, H. Jiang *et al.*, "The use of NH<sub>3</sub> to promote the production of large-diameter single-walled carbon nanotubes with a narrow (n,m) distribution," *J. Am. Chem. Soc.* **133**, 1224–1227 (2011).
- <sup>56</sup>B. C. Bayer, C. Baehtz *et al.*, "Nitrogen controlled iron catalyst phase during carbon nanotube growth," *Appl. Phys. Lett.* **105**, 143111 (2014).
- <sup>57</sup>D. Janas and K. K. Koziol, "Carbon nanotube fibers and films: Synthesis, applications and perspectives of the direct-spinning method," *Nanoscale* **8**, 19475–19490 (2016).
- <sup>58</sup>S. W. Pattinson, V. Ranganathan *et al.*, "Nitrogen-induced catalyst restructuring for epitaxial growth of multiwalled carbon nanotubes," *ACS Nano* **6**, 7723–7730 (2012).
- <sup>59</sup>R. M. Sundaram, K. K. K. Koziol *et al.*, "Continuous direct spinning of fibers of single-walled carbon nanotubes with metallic chirality," *Adv. Mater.* **23**, 5064–5068 (2011).
- <sup>60</sup>J. R. Sanchez-Valencia, T. Dienel *et al.*, "Controlled synthesis of single-chirality carbon nanotubes," *Nature* **512**, 61–64 (2014).
- <sup>61</sup>G. G. Samsonidze, S. G. Chou *et al.*, "Quantitative evaluation of the octadecylamine-assisted bulk separation of semiconducting and metallic single-wall carbon nanotubes by resonance Raman spectroscopy," *Appl. Phys. Lett.* **85**, 1006–1008 (2004).
- <sup>62</sup>G. P. Collins, "Engineering carbon nanotubes and nanotube circuits using electrical breakdown," *Science* **292**, 706–709 (2001).
- <sup>63</sup>A. Tunnell, V. Ballarotto *et al.*, "The selective removal of metallic carbon nanotubes from as-grown arrays on insulating substrates," *Appl. Phys. Lett.* **101**, 56–58 (2012).
- <sup>64</sup>K. Otsuka, T. Inoue *et al.*, "Selective removal of metallic single-walled carbon nanotubes in full length by organic film-assisted electrical breakdown," *Nanoscale* **6**, 8831–8835 (2014).
- <sup>65</sup>Z. Yongyi *et al.*, "Sorting out semiconducting single-walled carbon nanotube arrays by preferential destruction of metallic tubes using xenon-lamp irradiation," *J. Phys. Chem. C* **112**, 3849–3856 (2008).
- <sup>66</sup>H. Huang, R. Maruyama *et al.*, "Preferential destruction of metallic single-walled carbon nanotubes by laser irradiation," *J. Phys. Chem. B* **110**, 7316–7320 (2006).
- <sup>67</sup>M. S. Strano, "Probing chiral selective reactions using a revised Kataura plot for the interpretation of single-walled carbon nanotube spectroscopy," *J. Am. Chem. Soc.* **125**, 16148–16153 (2003).
- <sup>68</sup>M. Yudasaka, M. Zhang *et al.*, "Diameter-selective removal of single-wall carbon nanotubes through light-assisted oxidation," *Chem. Phys. Lett.* **374**, 132–136 (2003).
- <sup>69</sup>G. Zhang, P. Qi *et al.*, "Selective etching of metallic carbon nanotubes by gas-phase reaction," *Science* **314**, 974–977, (2006).
- <sup>70</sup>J. W. Song, H. W. Seo *et al.*, "Selective removal of metallic SWNTs using microwave radiation," *Curr. Appl. Phys.* **8**, 725–728 (2008).
- <sup>71</sup>B. R. Priya and H. J. Byrne, "Quantitative analyses of microwave-treated HiPco carbon nanotubes using absorption and Raman spectroscopy," *J. Phys. Chem. C* **113**, 7134–7138 (2009).
- <sup>72</sup>S. Nagasawa, M. Yudasaka *et al.*, "Effect of oxidation on single-wall carbon nanotubes," *Chem. Phys. Lett.* **328**, 374–380 (2000).
- <sup>73</sup>W. Zhou, Y. H. Ooi *et al.*, "Structural characterization and diameter-dependent oxidative stability of single wall carbon nanotubes synthesized by the catalytic decomposition of CO," *Chem. Phys. Lett.* **350**, 6–14 (2001).

- <sup>74</sup>M. S. Strano, C. A. Dyke *et al.*, “Electronic structure control of single-walled carbon nanotube functionalization,” *Science* **301**, 1519–1522, (2003).
- <sup>75</sup>C. Journet, W. K. Maser *et al.*, “Large-scale production of single-walled carbon nanotubes by the electric-arc technique,” *Nature* **388**, 756–758 (1997).
- <sup>76</sup>K. S. Kim, G. Cota-Sanchez *et al.*, “Large-scale production of single-walled carbon nanotubes by induction thermal plasma,” *J. Phys. D: Appl. Phys.* **40**, 2375–2387 (2007).
- <sup>77</sup>B. Kitiyanan, W. E. Alvarez *et al.*, “Controlled production of single-wall carbon nanotubes by catalytic decomposition of CO on bimetallic Co-Mo catalysts,” *Chem. Phys. Lett.* **317**, 497–503 (2000).
- <sup>78</sup>T. Lei, I. Pochorowski *et al.*, “Separation of semiconducting carbon nanotubes for flexible and stretchable electronics using polymer removable method,” *Acc. Chem. Res.* **50**, 1096–1104 (2017).
- <sup>79</sup>A. A. Green and M. C. Hersam, “Nearly single-chirality single-walled carbon nanotubes produced via orthogonal iterative density gradient ultracentrifugation,” *Adv. Mater.* **23**, 2185–2190 (2011).
- <sup>80</sup>S. K. Samanta, M. Fritsch *et al.*, “Conjugated polymer-assisted dispersion of single-wall carbon nanotubes: The power of polymer wrapping,” *Acc. Chem. Res.* **47**, 2446–2456 (2014).
- <sup>81</sup>A. Nish, J. Y. Hwang *et al.*, “Highly selective dispersion of single walled carbon nanotubes using aromatic polymers,” *Nat. Nanotechnol.* **2**, 640–646 (2007).
- <sup>82</sup>M. Zheng, A. Jagota *et al.*, “DNA-assisted dispersion and separation of carbon nanotubes,” *Nat. Mater.* **2**, 338–342 (2003).
- <sup>83</sup>H. P. Liu, D. Nishide *et al.*, “Large-scale single-chirality separation of single-wall carbon nanotubes by simple gel chromatography,” *Nat. Commun.* **2**, 309 (2011).
- <sup>84</sup>R. Krupke, F. Hennrich *et al.*, “Separation of metallic from semiconducting single-walled carbon nanotubes,” *Science* **301**, 344–347, (2003).
- <sup>85</sup>C. Y. Khrapin, J. A. Fagan *et al.*, “Spontaneous partition of carbon nanotubes in polymer-modified aqueous phases,” *J. Am. Chem. Soc.* **135**, 6822–6825 (2013).
- <sup>86</sup>L. Y. Liang, W. Y. Xie *et al.*, “High-efficiency dispersion and sorting of single-walled carbon nanotubes via non-covalent interactions,” *J. Mater. Chem. C* **5**, 11339–11368 (2017).
- <sup>87</sup>M. S. Arnold, A. A. Green *et al.*, “Sorting carbon nanotubes by electronic structure using density differentiation,” *Nat. Nanotechnol.* **1**, 60–65 (2006).
- <sup>88</sup>X. M. Tu, S. Manohar *et al.*, “DNA sequence motifs for structure-specific recognition and separation of carbon nanotubes,” *Nature* **460**, 250–253 (2009).
- <sup>89</sup>Q. Cao, S. J. Han *et al.*, “Fringing-field dielectrophoretic assembly of ultrahigh-density semiconducting nanotube arrays with a self-limited pitch,” *Nat. Commun.* **5**, 5071 (2014).
- <sup>90</sup>H. Li, G. Gordeev *et al.*, “Separation of small-diameter single-walled carbon nanotubes in one to three steps with aqueous two-phase extraction,” *ACS Nano* **13**, 2567–2578 (2019).
- <sup>91</sup>S. Qiu, K. J. Wu *et al.*, “Solution-processing of high-purity semiconducting single-walled carbon nanotubes for electronics devices,” *Adv. Mater.* **31**, 1970063 (2019).
- <sup>92</sup>G. S. Tulevski, A. D. Franklin *et al.*, “High purity isolation and quantification of semiconducting carbon nanotubes via column chromatography,” *ACS Nano* **7**, 2971–2976 (2013).
- <sup>93</sup>D. H. Yang, L. H. Li *et al.*, “Submilligram-scale separation of near-zigzag single-chirality carbon nanotubes by temperature controlling a binary surfactant system,” *Sci. Adv.* **7**, eabe0084 (2021).
- <sup>94</sup>S. Zanoni, B. P. Watts *et al.*, “Single-walled carbon nanotube chiral selectivity exhibited by commercially available hydrogels of varying composition,” *ACS Appl. Mater. Interfaces* **13**, 33635–33643 (2021).
- <sup>95</sup>M. Dolan, B. P. Watts *et al.*, “Tailored synthesis of hydrogel media for chirality separation of single walled carbon nanotubes,” *Carbon* **171**, 597–609 (2021).
- <sup>96</sup>X. Luo, X. J. Wei *et al.*, “One-step separation of high-purity single-chirality single-wall carbon nanotubes using sodium hyodeoxycholate,” *Carbon* **207**, 129–135 (2023).
- <sup>97</sup>S. Mesgari, A. K. Sundramoorthy *et al.*, “Gel electrophoresis using a selective radical for the separation of single-walled carbon nanotubes,” *Faraday Discuss.* **173**, 351–363 (2014).
- <sup>98</sup>X. Z. Xu, Z. Mukadam *et al.*, “Directed assembly of multiplexed single chirality carbon nanotube devices,” *J. Appl. Phys.* **129**, 024305 (2021).
- <sup>99</sup>B. Podlesny, B. Olszewska *et al.*, “En route to single-step, two-phase purification of carbon nanotubes facilitated by high-throughput spectroscopy,” *Sci. Rep.* **11**, 10618 (2021).
- <sup>100</sup>B. Podlesny, K. R. Hinkle *et al.*, “Highly-selective harvesting of (6,4) SWCNTs using the aqueous two-phase extraction method and nonionic surfactants,” *Adv. Sci.* **10**, 2207218 (2023).
- <sup>101</sup>V. A. Eremina, P. A. Obraztsov *et al.*, “Separation and optical identification of semiconducting and metallic single-walled carbon nanotubes,” *Phys. Status Solidi B* **254**, 1600659 (2017).
- <sup>102</sup>N. K. Subbaian, A. N. G. Parra-Vasquez *et al.*, “Bench-top aqueous two-phase extraction of isolated individual single-walled carbon nanotubes,” *Nano Res.* **8**, 1755–1769 (2015).
- <sup>103</sup>J. L. Feng, S. M. Alam *et al.*, “Sorting of single-walled carbon nanotubes based on metallicity by selective precipitation with polyvinylpyrrolidone,” *J. Phys. Chem. C* **115**, 5199–5206 (2011).
- <sup>104</sup>J. A. Fagan, E. H. Haroz *et al.*, “Isolation of >1 nm diameter single-wall carbon nanotube species using aqueous two-phase extraction,” *ACS Nano* **9**, 5377–5390 (2015).
- <sup>105</sup>J. A. Fagan, C. Y. Khrapin *et al.*, “Isolation of specific small-diameter single-wall carbon nanotube species via aqueous two-phase extraction,” *Adv. Mater.* **26**, 2800–2804 (2014).
- <sup>106</sup>M. Rother, S. P. Schiessi *et al.*, “Understanding charge transport in mixed networks of semiconducting carbon nanotubes,” *ACS Appl. Mater. Interfaces* **8**, 5571–5579 (2016).
- <sup>107</sup>Y. Kanai and J. C. Grossman, “Role of semiconducting and metallic tubes in P3HT/carbon-nanotube photovoltaic heterojunctions: Density functional theory calculations,” *Nano Lett.* **8**, 908–912 (2008).
- <sup>108</sup>H. L. Wang, B. Hsieh *et al.*, “Solvent effects on polymer sorting of carbon nanotubes with applications in printed electronics,” *Small* **11**, 126–133 (2015).
- <sup>109</sup>H. L. Wang and Z. N. Bao, “Conjugated polymer sorting of semiconducting carbon nanotubes and their electronic applications,” *Nano Today* **10**, 737–758 (2015).
- <sup>110</sup>J. T. Gu, J. Han *et al.*, “Solution-processable high-purity semiconducting SWCNTs for large-area fabrication of high-performance thin-film transistors,” *Small* **12**, 4993–4999 (2016).
- <sup>111</sup>F. Lemasson, J. Tittmann *et al.*, “Debundling, selection and release of SWNTs using fluorene-based photocleavable polymers,” *Chem. Commun.* **47**, 7428–7430 (2011).
- <sup>112</sup>Z. Li, J. F. Ding *et al.*, “Decomposable s-tetrazine copolymer enables single-walled carbon nanotube thin film transistors and sensors with improved sensitivity,” *Adv. Funct. Mater.* **28**, 1705568 (2018).
- <sup>113</sup>I. Pochorowski, H. L. Wang *et al.*, “H-bonded supramolecular polymer for the selective dispersion and subsequent release of large-diameter semiconducting single-walled carbon nanotubes,” *J. Am. Chem. Soc.* **137**, 4328–4331 (2015).
- <sup>114</sup>F. Toshimitsu and N. Nakashima, “Semiconducting single-walled carbon nanotubes sorting with a removable solubilizer based on dynamic supramolecular coordination chemistry,” *Nat. Commun.* **5**, 5041 (2014).
- <sup>115</sup>W. Z. Wang, W. F. Li *et al.*, “Degradable conjugated polymers: Synthesis and applications in enrichment of semiconducting single-walled carbon nanotubes,” *Adv. Funct. Mater.* **21**, 1643–1651 (2011).
- <sup>116</sup>D. J. Hill and J. S. Moore, “Helicogenicity of solvents in the conformational equilibrium of oligo(m-phenylene ethynylene)s: Implications for foldamer research,” *Proc. Natl. Acad. Sci. U.S.A.* **99**, 5053–5057 (2002).
- <sup>117</sup>S. Liang, G. Chen *et al.*, “Conformationally switchable TTFV-phenylacetylene polymers: Synthesis, properties, and supramolecular interactions with single-walled carbon nanotubes,” *J. Mater. Chem. C* **1**, 5477–5490 (2013).
- <sup>118</sup>Y. Joo, G. J. Brady *et al.*, “Isolation of pristine electronics grade semiconducting carbon nano tubes by switching the rigidity of the wrapping polymer backbone on demand,” *ACS Nano* **9**, 10203–10213 (2015).
- <sup>119</sup>S. Liang, Y. M. Zhao *et al.*, “Selective and reversible noncovalent functionalization of single-walled carbon nanotubes by a pH-responsive vinyllogous tetrathiafulvalene-fluorene copolymer,” *J. Am. Chem. Soc.* **136**, 970–977 (2014).

- <sup>120</sup>G. Hills, C. Lau *et al.*, "Modern microprocessor built from complementary carbon nanotube transistors," *Nature* **572**, 595–602 (2019).
- <sup>121</sup>L. J. Liu, J. Han *et al.*, "Aligned, high-density semiconducting carbon nanotube arrays for high-performance electronics," *Science* **368**, 850–856, (2020).
- <sup>122</sup>F. Liu, X. X. Chen *et al.*, "Comparative study of the extraction selectivity of PFO-BPy and PCz for small to large diameter single-walled carbon nanotubes," *Nano Res.* **15**, 8479–8485 (2022).
- <sup>123</sup>H. Ozawa, N. Ide *et al.*, "One-pot separation of highly enriched (6,5)-single-walled carbon nanotubes using a fluorene-based copolymer," *Chem. Lett.* **40**, 239–241 (2011).
- <sup>124</sup>J. Y. Ouyang, H. Shin *et al.*, "Impact of conjugated polymer characteristics on the enrichment of single-chirality single-walled carbon nanotubes," *ACS Appl. Polym. Mater.* **4**, 6239–6254 (2022).
- <sup>125</sup>T. Lei, Y. C. Lai *et al.*, "Diketopyrrolopyrrole (DPP)-based donor-acceptor polymers for selective dispersion of large-diameter semiconducting carbon nanotubes," *Small* **11**, 2946–2954 (2015).
- <sup>126</sup>Y. H. Li, M. M. Zheng *et al.*, "High-purity monochiral carbon nanotubes with a 1.2 nm diameter for high-performance field-effect transistors," *Adv. Funct. Mater.* **32**, 2107119 (2022).
- <sup>127</sup>H. Ozawa, T. Fujigaya *et al.*, "Rational concept to recognize/extract single-walled carbon nanotubes with a specific chirality," *J. Am. Chem. Soc.* **133**, 2651–2657 (2011).
- <sup>128</sup>N. Sturzl, F. Hennrich *et al.*, "Near monochiral single-walled carbon nanotube dispersions in organic solvents," *J. Phys. Chem. C* **113**, 14628–14632 (2009).
- <sup>129</sup>M. Brohmann, M. Rother *et al.*, "Temperature-dependent charge transport in polymer-sorted semiconducting carbon nanotube networks with different diameter distributions," *J. Phys. Chem. C* **122**, 19886–19896 (2018).
- <sup>130</sup>J. Yao, Y. J. Li *et al.*, "Rapid annealing and cooling induced surface cleaning of semiconducting carbon nanotubes for high-performance thin-film transistors," *Carbon* **184**, 764–771 (2021).
- <sup>131</sup>F. Bottacchi, L. Petti *et al.*, "Polymer-sorted (6,5) single-walled carbon nanotubes for solution-processed low-voltage flexible microelectronics," *Appl. Phys. Lett.* **106**, 193302 (2015).
- <sup>132</sup>L. Wieland, H. Li *et al.*, "Carbon nanotubes for photovoltaics: From lab to industry," *Adv. Energy Mater.* **11**, 2170014 (2021).
- <sup>133</sup>F. M. Chen, B. Wang *et al.*, "Toward the extraction of single species of single-walled carbon nanotubes using fluorene-based polymers," *Nano Lett.* **7**, 3013–3017 (2007).
- <sup>134</sup>M. Tange, T. Okazaki *et al.*, "Selective extraction of large-diameter single-wall carbon nanotubes with specific chiral indices by poly(9,9-diethylfluorene-alt-benzothiadiazole)," *J. Am. Chem. Soc.* **133**, 11908–11911 (2011).
- <sup>135</sup>M. Tange, T. Okazaki *et al.*, "Selective extraction of semiconducting single-wall carbon nanotubes by poly(9,9-diethylfluorene-alt-pyridine) for 1.5 μm emission," *ACS Appl. Mater. Interfaces* **4**, 6458–6462 (2012).
- <sup>136</sup>Y. H. Li, M. M. Zheng *et al.*, "High-purity monochiral carbon nanotubes with a 1.2 nm diameter for high-performance field-effect transistors," *Adv. Funct. Mater.* **32**, 2107119 (2022).
- <sup>137</sup>J. F. Ding, Z. Li *et al.*, "Enrichment of large-diameter semiconducting SWCNTs by polyfluorene extraction for high network density thin film transistors," *Nanoscale* **6**, 2328–2339 (2014).
- <sup>138</sup>K. S. Mistry, B. A. Larsen *et al.*, "High-yield dispersions of large-diameter semiconducting single-walled carbon nanotubes with tunable narrow chirality distributions," *ACS Nano* **7**, 2231–2239 (2013).
- <sup>139</sup>H. Shi, L. Ding *et al.*, "Radiofrequency transistors based on aligned carbon nanotube arrays," *Nat. Electron.* **4**, 405–415 (2021).
- <sup>140</sup>G. J. Brady, Y. Joo *et al.*, "High performance transistors via aligned polyfluorene-sorted carbon nanotubes," *Appl. Phys. Lett.* **104**, 083107 (2014).
- <sup>141</sup>B. Gao, X. Zhang *et al.*, "Assembly of aligned semiconducting carbon nanotubes in organic solvents via introducing inter-tube electrostatic repulsion," *Carbon* **146**, 172–180 (2019).
- <sup>142</sup>I. Yu, Y. Ye *et al.*, "A bendable, stretchable transistor with aligned carbon nanotube films," *Adv. Mater. Interfaces* **6**, 1900945 (2019).
- <sup>143</sup>Z. Zhang, S. Wang *et al.*, "Self-aligned ballistic n-type single-walled carbon nanotube field-effect transistors with adjustable threshold voltage," *Nano Lett.* **8**, 3696 (2008).
- <sup>144</sup>G. J. Brady, Y. Joo *et al.*, "Polyfluorene-sorted, carbon nanotube array field-effect transistors with increased current density and high on/off ratio," *ACS Nano* **8**, 11614–11621 (2014).
- <sup>145</sup>V. Derenskyi, W. Gomulya *et al.*, "Carbon nanotube network ambipolar field-effect transistors with 10(8) on/off ratio," *Adv. Mater.* **26**, 5969–5975 (2014).
- <sup>146</sup>W. J. Xu, M. Li *et al.*, "Printed thin film transistors with 10(8) on/off ratios and photoelectrical synergistic characteristics using isoindigo-based polymers-enriched (9,8) carbon nanotubes," *Nano Res.* **15**, 5517–5526 (2022).
- <sup>147</sup>F. Hennrich, W. S. Li *et al.*, "Length-sorted, large-diameter, polyfluorene-wrapped semiconducting single-walled carbon nanotubes for high-density, short-channel transistors," *ACS Nano* **10**, 1888–1895 (2016).
- <sup>148</sup>X. He, H. Htoon *et al.*, "Carbon nanotubes as emerging quantum-light sources," *Nat. Mater.* **17**, 663–670 (2018).
- <sup>149</sup>X. W. He, F. Leonard *et al.*, "Uncooled carbon nanotube photodetectors," *Adv. Opt. Mater.* **3**, 989–1011 (2015).
- <sup>150</sup>W. A. G. Rojas and M. C. Hersam, "Chirality-enriched carbon nanotubes for next-generation computing," *Adv. Mater.* **32**, 1905654 (2020).
- <sup>151</sup>M. Brohmann, F. J. Berger *et al.*, "Charge transport in mixed semiconducting carbon nanotube networks with tailored mixing ratios," *ACS Nano* **13**, 7323–7332 (2019).
- <sup>152</sup>W. Su, D. H. Yang *et al.*, "Ultrafast wafer-scale assembly of uniform and highly dense semiconducting carbon nanotube films for optoelectronics," *Carbon* **163**, 370–378 (2020).
- <sup>153</sup>Z. H. Chen, J. Appenzeller *et al.*, "The role of metal-nanotube contact in the performance of carbon nanotube field-effect transistors," *Nano Lett.* **5**, 1497–1502 (2005).
- <sup>154</sup>Y. J. Zhao, D. Candebat *et al.*, "Understanding the impact of Schottky barriers on the performance of narrow bandgap nanowire field effect transistors," *Nano Lett.* **12**, 5331–5336 (2012).
- <sup>155</sup>G. S. Tulevski, A. D. Franklin *et al.*, "Toward high-performance digital logic technology with carbon nanotubes," *ACS Nano* **8**, 8730–8745 (2014).
- <sup>156</sup>W. Gomulya, G. D. Costanzo *et al.*, "Semiconducting single-walled carbon nanotubes on demand by polymer wrapping," *Adv. Mater.* **25**, 2948–2956 (2013).
- <sup>157</sup>X. S. Yang, T. H. Liu *et al.*, "Host-guest molecular interaction enabled separation of large-diameter semiconducting single-walled carbon nanotubes," *J. Am. Chem. Soc.* **143**, 10120–10130 (2021).
- <sup>158</sup>L. Zhang, X. Tu *et al.*, "Optical characterizations and electronic devices of nearly pure (10,5) single-walled carbon nanotubes," *J. Am. Chem. Soc.* **131**, 2454–2455 (2009).
- <sup>159</sup>H. J. Wen, J. Yao *et al.*, "Length-dependent alignment of large-area semiconducting carbon nanotubes self-assembly on a liquid-liquid interface," *Nano Res.* **16**, 1568–1575 (2023).
- <sup>160</sup>J. Yao, Q. Song, H. H. Jin, and Q. W. Li, "Research on length sorting of semiconducting carbon nanotubes and the performance of thin film transistors," *Semicond. Optoelectron.* **42**, 348–352 (2021).
- <sup>161</sup>X. W. He, W. L. Gao *et al.*, "Wafer-scale monodomain films of spontaneously aligned single-walled carbon nanotubes," *Nat. Nanotechnol.* **11**, 633–638 (2016).
- <sup>162</sup>L. Wei, B. L. Liu *et al.*, "(9,8) single-walled carbon nanotube enrichment via aqueous two-phase separation and their thin-film transistor applications," *Adv. Electron. Mater.* **1**, 1500151 (2015).
- <sup>163</sup>M. M. Zheng, Y. H. Li, J. Yao, Q. Song, H. H. Jin K, J. Wu, D. D. Liu, and Q. W. Li, "Research on separation of different chiral single-walled carbon nanotube and the performance of field effect transistors," *Semicond. Optoelectron.* **41**, 344–350 (2021).
- <sup>164</sup>P. H. Lau, K. Takei *et al.*, "Fully printed, high performance carbon nanotube thin-film transistors on flexible substrates," *Nano Lett.* **13**, 3864–3869 (2013).
- <sup>165</sup>M. Rother, M. Brohmann *et al.*, "Aerosol-jet printing of polymer-sorted (6,5) carbon nanotubes for field-effect transistors with high reproducibility," *Adv. Electron. Mater.* **3**, 1700080 (2017).

- <sup>166</sup>V. Perebeinos, J. Tersoff *et al.*, “Electron-phonon interaction and transport in semiconducting carbon nanotubes,” *Phys. Rev. Lett.* **94**, 086802 (2005).
- <sup>167</sup>X. J. Zhou, J. Y. Park *et al.*, “Band structure, phonon scattering, and the performance limit of single-walled carbon nanotube transistors,” *Phys. Rev. Lett.* **95**, 146805 (2005).
- <sup>168</sup>I. S. Esqueda, X. D. Yan *et al.*, “Aligned carbon nanotube synaptic transistors for large-scale neuromorphic computing,” *ACS Nano* **12**, 7352–7361 (2018).
- <sup>169</sup>T. Hertel, R. Martel *et al.*, “Manipulation of individual carbon nanotubes and their interaction with surfaces,” *J. Phys. Chem. B* **102**, 910–915 (1998).
- <sup>170</sup>M. Kawai, H. Kyakuno *et al.*, “Single chirality extraction of single-wall carbon nanotubes for the encapsulation of organic molecules,” *J. Am. Chem. Soc.* **134**, 9545–9548 (2012).
- <sup>171</sup>S. G. Noyce, J. L. Doherty *et al.*, “Electronic stability of carbon nanotube transistors under long-term bias stress,” *Nano Lett.* **19**, 1460–1466 (2019).
- <sup>172</sup>D. Zhong, H. Shi *et al.*, “Carbon nanotube film-based radio frequency transistors with maximum oscillation frequency above 100 GHz,” *ACS Appl. Mater. Interfaces* **11**, 42496–42503 (2019).
- <sup>173</sup>X. Y. Liu, B. Sun *et al.*, “Floating gate carbon nanotube dual-gate field-effect transistor for reconfigurable AND/OR logic gates,” *ACS Appl. Electron. Mater.* **4**, 1684–1691 (2022).
- <sup>174</sup>Z. Y. Zhang, X. L. Liang *et al.*, “Doping-free fabrication of carbon nanotube based ballistic CMOS devices and circuits,” *Nano Lett.* **7**, 3603–3607 (2007).
- <sup>175</sup>C. Liu, Y. Cao *et al.*, “Complementary transistors based on aligned semiconducting carbon nanotube arrays,” *ACS Nano* **16**, 21482–21490 (2022).
- <sup>176</sup>H. W. Shi, L. Ding *et al.*, “Deep-submicrometer complementary metal-oxide-semiconductor transistors based on carbon nanotube films,” *Adv. Electron. Mater.* **8**, 2100751 (2022).
- <sup>177</sup>M. Hartmann, S. Hermann *et al.*, “CNTFET technology for RF applications: Review and future perspective,” *IEEE J. Microw.* **1**, 275–287 (2021).
- <sup>178</sup>A. Javey, J. Guo *et al.*, “High-field quasiballistic transport in short carbon nanotubes,” *Phys. Rev. Lett.* **92**, 4 (2004).
- <sup>179</sup>J. M. Bethoux, H. Happy *et al.*, “An 8-GHz f/sub t/ carbon nanotube field-effect transistor for gigahertz range applications,” *IEEE Electron Device Lett.* **27**, 681–683 (2006).
- <sup>180</sup>A. Le Louarn, F. Kapche *et al.*, “Intrinsic current gain cutoff frequency of 30 GHz with carbon nanotube transistors,” *Appl. Phys. Lett.* **90**, 3 (2007).
- <sup>181</sup>L. Nougaret, H. Happy *et al.*, “80 GHz field-effect transistors produced using high purity semiconducting single-walled carbon nanotubes,” *Appl. Phys. Lett.* **94**, 3 (2009).
- <sup>182</sup>Y. C. Che, A. Badmaev *et al.*, “Self-aligned T-gate high-purity semiconducting carbon nanotube RF transistors operated in quasi-ballistic transport and quantum capacitance regime,” *ACS Nano* **6**, 6936–6943 (2012).
- <sup>183</sup>Y. Cao, Y. C. Che *et al.*, “Radio frequency transistors based on ultra-high purity semiconducting carbon nanotubes with superior extrinsic maximum oscillation frequency,” *Nano Res.* **9**, 363–371 (2016).
- <sup>184</sup>Y. Cao, Y. C. Che *et al.*, “High-performance radio frequency transistors based on diameter-separated semiconducting carbon nanotubes,” *Appl. Phys. Lett.* **108**, 233105 (2016).
- <sup>185</sup>J. S. Zhou, L. J. Liu *et al.*, “Carbon nanotube based radio frequency transistors for K-band amplifiers,” *ACS Appl. Mater. Interfaces* **13**, 37475–37482 (2021).
- <sup>186</sup>S. J. Kang, C. Kocabas, T. Ozel *et al.*, “High-performance electronics using dense, perfectly aligned arrays of single-walled carbon nanotubes,” *Nat. Nanotechnol.* **2**, 230–236 (2007).
- <sup>187</sup>C. Kocabas, S. Dunham *et al.*, “High-frequency performance of submicrometer transistors that use aligned arrays of single-walled carbon nanotubes,” *Nano Lett.* **9**, 1937–1943 (2009).
- <sup>188</sup>M. Steiner, M. Engel *et al.*, “High-frequency performance of scaled carbon nanotube array field-effect transistors,” *Appl. Phys. Lett.* **101**, 053123 (2012).
- <sup>189</sup>Y. C. Che, Y. C. Lin *et al.*, “T-gate aligned nanotube radio frequency transistors and circuits with superior performance,” *ACS Nano* **7**, 4343–4350 (2013).
- <sup>190</sup>Y. Cao, G. J. Brady *et al.*, “Radio frequency transistors using aligned semiconducting carbon nanotubes with current-gain cutoff frequency and maximum oscillation frequency simultaneously greater than 70 GHz,” *ACS Nano* **10**, 6782–6790 (2016).
- <sup>191</sup>C. Rutherglen, A. A. Kane *et al.*, “Wafer-scalable, aligned carbon nanotube transistors operating at frequencies of over 100 GHz,” *Nat. Electron.* **2**, 530–539 (2019).
- <sup>192</sup>S. J. Kang, C. Kocabas *et al.*, “High-performance electronics using dense, perfectly aligned arrays of single-walled carbon nanotubes,” *Nat. Nanotechnol.* **2**, 230–236 (2007).
- <sup>193</sup>S. Kim, H. J. Kwon *et al.*, “Low-power flexible organic light-emitting diode display device,” *Adv. Mater.* **23**, 3511–3516 (2011).
- <sup>194</sup>B. Yoon, D. Y. Ham *et al.*, “Inkjet printing of conjugated polymer precursors on paper substrates for colorimetric sensing and flexible electrothermochromic display,” *Adv. Mater.* **23**, 5492–5497 (2011).
- <sup>195</sup>W. Gao, S. Emaminejad *et al.*, “Fully integrated wearable sensor arrays for multiplexed *in situ* perspiration analysis,” *Nature* **529**, 509–514 (2016).
- <sup>196</sup>L. Y. Chen, B. C. K. Tee *et al.*, “Continuous wireless pressure monitoring and mapping with ultra-small passive sensors for health monitoring and critical care,” *Nat. Commun.* **5**, 5028 (2014).
- <sup>197</sup>Y. Khan, A. E. Ostfeld *et al.*, “Monitoring of vital signs with flexible and wearable medical devices,” *Adv. Mater.* **28**, 4373–4395 (2016).
- <sup>198</sup>H. Fang, K. J. Yu *et al.*, “Capacitively coupled arrays of multiplexed flexible silicon transistors for long-term cardiac electrophysiology,” *Nat. Biomed. Eng.* **1**, 1 (2017).
- <sup>199</sup>L. Xiang, H. Zhang *et al.*, “Carbon nanotube-based flexible electronics,” *J. Mater. Chem. C* **6**, 7714–7727 (2018).
- <sup>200</sup>Q. Cao, H. S. Kim *et al.*, “Medium-scale carbon nanotube thin-film integrated circuits on flexible plastic substrates,” *Nature* **454**, 495–500 (2008).
- <sup>201</sup>C. X. Zhu, A. Chortos *et al.*, “Stretchable temperature-sensing circuits with strain suppression based on carbon nanotube transistors,” *Nat. Electron.* **1**, 183–190 (2018).
- <sup>202</sup>J. S. Tang, Q. Cao *et al.*, “Flexible CMOS integrated circuits based on carbon nanotubes with sub-10 ns stage delays,” *Nat. Electron.* **1**, 191–196 (2018).
- <sup>203</sup>D. Kiriya, K. Chen *et al.*, “Design of surfactant-substrate interactions for roll-to-roll assembly of carbon nanotubes for thin-film transistors,” *J. Am. Chem. Soc.* **136**, 11188–11194 (2014).
- <sup>204</sup>J. L. Chen, S. Mishra *et al.*, “Thin dielectric-layer-enabled low-voltage operation of fully printed flexible carbon nanotube thin-film transistors,” *Nanotechnology* **31**, 235301 (2020).
- <sup>205</sup>T. Y. Qu, Y. Sun *et al.*, “A flexible carbon nanotube sen-memory device,” *Adv. Mater.* **32**, 1907288 (2020).
- <sup>206</sup>X. Q. Li, Y. F. Ren *et al.*, “A universal method for high-efficiency immobilization of semiconducting carbon nanotubes toward fully printed paper-based electronics,” *Adv. Electron. Mater.* **7**, 200125 (2021).
- <sup>207</sup>G. H. Long, W. L. Jin *et al.*, “Carbon nanotube-based flexible high-speed circuits with sub-nanosecond stage delays,” *Nat. Commun.* **13**, 6734 (2022).
- <sup>208</sup>Y. Sun, P. P. Li *et al.*, “Key factors for ultra-high on/off ratio thin-film transistors using as-grown carbon nanotube networks,” *RSC Adv.* **12**, 16291–16295 (2022).
- <sup>209</sup>X. Q. Li, S. Jiang *et al.*, “Preparation of isolated semiconducting single-wall carbon nanotubes by oxygen-assisted floating catalyst chemical vapor deposition,” *Chem. Eng. J.* **450**, 137861 (2022).
- <sup>210</sup>J. Q. Li, M. Li *et al.*, “Large area roll-to-roll printed semiconducting carbon nanotube thin films for flexible carbon-based electronics,” *Nanoscale* **15**, 5317–5326 (2023).
- <sup>211</sup>G. H. Long, W. L. Jin *et al.*, “Carbon nanotube-based flexible high-speed circuits with sub-nanosecond stage delays,” *Nat. Commun.* **13**, 6734 (2022).
- <sup>212</sup>M. M. Slepchenkov, P. V. Barkov *et al.*, “Island-type graphene-nanotube hybrid structures for flexible and stretchable electronics: In silico study,” *Micromachines* **14**, 671 (2023).